

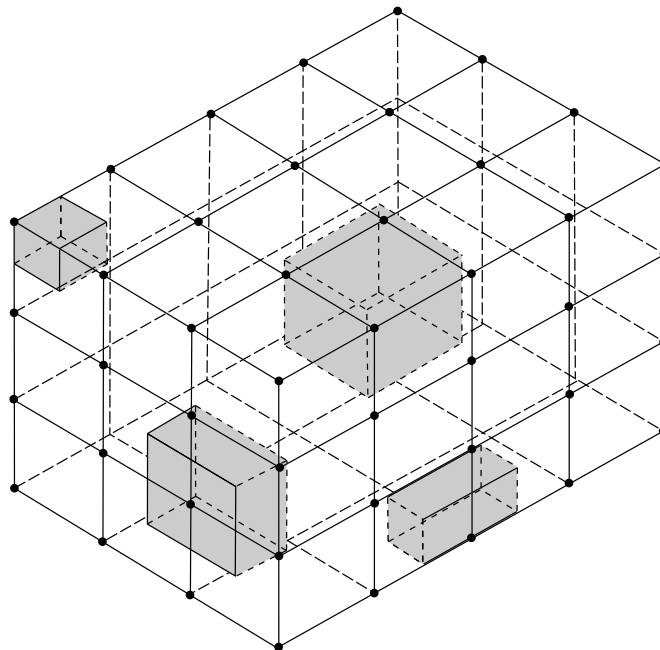
Simulation of Subsurface Storage and Recovery of Effluent Using Multiple Wells, St. Petersburg, Florida

U.S. Geological Survey

Water-Resources Investigations Report 97-4024

Prepared in cooperation with the

City of St. Petersburg and the
Southwest Florida Water Management District



Cover: Sketch of finite-difference spatial discretization for a cartesian-coordinate system.

Simulation of Subsurface Storage and Recovery of Effluent Using Multiple Wells, St. Petersburg, Florida

By Dann K. Yobbi

U.S. GEOLOGICAL SURVEY

Water-Resources Investigations Report 97-4024

Prepared in cooperation with the

CITY OF ST. PETERSBURG and the
SOUTHWEST FLORIDA WATER MANAGEMENT DISTRICT

Tallahassee, Florida
1997



U.S. DEPARTMENT OF THE INTERIOR

BRUCE BABBITT, Secretary

U.S. GEOLOGICAL SURVEY

Gordon P. Eaton, Director

Any use of trade, product, or firm names in this publication is for descriptive purposes only and does not imply endorsement by the U.S. Geological Survey.

For additional information write to:

District Chief
U.S. Geological Survey
227 North Bronough Street, Suite 3015
Tallahassee, Florida 32301

Copies of this report can be
purchased from:

U.S. Geological Survey
Branch of Information Center
Box 25286
Denver, CO 80225-0425

CONTENTS

- Abstract..... 1
- Introduction 2
 - Purpose and Scope..... 2
 - Description of Study Site..... 3
 - Subsurface Storage and Recovery Concept..... 4
 - Factors Affecting Recovery Efficiency 4
- Hydrogeologic Framework..... 5
- Numerical Analysis of Hydraulic Properties 6
 - Model Grid and Boundary Conditions 8
 - Calibration 8
 - Sensitivity Analysis..... 9
 - Hydraulic Conductivity 10
 - Matrix Compressibility..... 13
- Simulation of Subsurface Storage and Recovery of Effluent Using Multiple Wells..... 13
 - Numerical Model..... 14
 - Design of Base Model 14
 - Grid Design..... 15
 - Boundary Conditions..... 16
 - Fluid Properties..... 16
 - Matrix Properties 17
 - Effects of Operational Factors on Recovery Efficiency 18
 - Base Simulation..... 18
 - Multiple-Well Configurations..... 21
 - Rates of Injection and Recovery..... 22
 - Volume of Water Injected 23
 - Storage Time and Regional Flow 23
 - Successive Cycles of Injection and Recovery 24
 - Sensitivity Analysis 24
 - Dissolved-Solids Concentration of the Injection Zone..... 26
 - Permeability..... 26
 - Anisotropy 28
 - Dispersivity..... 28
 - Effective Porosity 28
- Summary and Conclusions 29
- Selected References 30

FIGURES

- 1. Map showing location of study area and the city of St. Petersburg injection sites 3
- 2. Generalized stratigraphic and hydrogeologic section, St. Petersburg, Florida..... 5
- 3. Generalized hydrogeologic section and configuration of test and observation wells..... 7
- 4. Cylindrical-model grid used for the simulation of hydraulic properties of the aquifer system at the Southwest St. Petersburg Water Reclamation Facility 8
- 5. Simulated and observed drawdowns in wells B-9, B-5, and B-4 9
- 6. Simulated flow field at the end of the 3.45 day aquifer test 10

7-8. Graphs showing:	
7. Effects of varying hydraulic conductivity on the simulated drawdowns in semiconfining unit between zones A and B, zone A lower unit, and zone A upper unit	11
8. Effects of varying matrix compressibility on the simulated drawdowns in semiconfining unit between zones A and B, zone A lower unit, and zone A upper unit	12
9. Vertical and horizontal discretization of the model grid used for the simulation of subsurface storage and recovery	15
10. Simulated flow field along vertical plane 16 at the end of the injection and recovery phases of the base simulation	19
11. Simulated dissolved-solids concentration along vertical plane 16 at the end of the injection and recovery phases of the base simulation	20
12. Geometric arrangement of injection and recovery wells.....	22
13. Simulated flow field along vertical plane 16 at the end of 30, 180, and 360 days of storage	25
14-15. Graphs showing:	
14. Recovery efficiency for ten successive injection/withdrawal cycles at 4.0 million gallons per day.....	26
15. Relation between recovery efficiency and variations in selected model parameters	27

TABLES

1. Fluid properties assumed for simulation.....	17
2. Matrix properties assumed for simulation	17

CONVERSION FACTORS AND ABBREVIATIONS

Multiply inch-pound unit	By	To obtain
foot (ft)	0.3048	meter
mile (mi)	1.6090	kilometer
foot squared (ft ²)	0.0920	meter squared
foot per day (ft/d)	0.3048	meter per day
foot per mile (ft/mi)	0.1894	meter per kilometer
foot squared per day (ft ² /d)	0.0920	square meter
gallon per minute (gal/min)	0.0631	liters per second
inch per year (in/yr)	25.4	millimeter per year
pounds per square inch (lb/in ²)	6.8950	kilopascal
pounds per cubic foot (lb/ft ³)	0.0160	grams per cubic centimeter
million gallons per day (Mgal/d)	0.4381	cubic meter per day

Equation for temperature conversion between degrees Celsius (°C) and degrees Fahrenheit (°F):

$$^{\circ}\text{C} = 5/9 \times (^{\circ}\text{F} - 32)$$

$$^{\circ}\text{F} = (9/5 \text{ } ^{\circ}\text{C}) + 32$$

Milligrams per liter (mg/L) is a unit expressing the concentration of chemical constituents in solution as weight (milligrams) of solute per unit volume (liter) of water. For concentrations less than 7,000 mg/L, the numerical value is the same as for concentrations in parts per million.

Sea level: In this report, “sea level” refers to the National Geodetic Vertical Datum of 1929 (NGVD of 1929)---a geodetic datum derived from a general adjustment of the first-order level nets of the United States and Canada, formerly called “Sea Level Datum of 1929.”

ADDITIONAL ABBREVIATIONS

α_T	transverse dispersivity
α_L	longitudinal dispersivity
k_h	horizontal permeability
k_v	vertical permeability
C_r	rock compressibility
Q_r	recovery rate
Q	injection rate
S	storage coefficient

ACRONYMS USED IN THIS REPORT:

DS	dissolved solids
HST3D	U.S. Geological Survey Three Dimensional Heat- and Solute-Transport computer program
I	intermediate confining unit
C	
U	
SCU A/B	semiconfining unit between zones A and B
SSMF	scaled-solute mass fraction
SSR	subsurface storage and recovery
SWFWMD	Southwest Florida Water Management District
UFA	Upper Floridan aquifer
USGS	U.S. Geological Survey
WRF	water reclamation facilities

Simulation of Subsurface Storage and Recovery of Effluent Using Multiple Wells, St. Petersburg, Florida

By Dann K. Yobbi

Abstract

The potential for subsurface storage and recovery, otherwise called aquifer storage and recovery, of effluent in the uppermost producing zone of the Upper Floridan aquifer in St. Petersburg, Florida, was studied by the U.S. Geological Survey, in cooperation with the city of St. Petersburg and the Southwest Florida Water Management District. The success of subsurface storage and recovery depends on the recovery efficiency, or the quantity of water, relative to the quantity injected, that can be recovered before the water that is withdrawn fails to meet salinity limits. The viability of this practice will depend upon the ability of the injected zone to receive, store, and discharge the injected fluid.

A three-dimensional numerical model of ground-water flow and solute transport, incorporating available data on aquifer properties and water quality, was developed to evaluate the effects of changing various operational factors on recovery efficiency. The reference case for testing was a base model considered representative of the aquifer system underlying the Southwest St. Petersburg Water Treatment Facility. The base simulation used as a standard for comparison consisted of a single cycle of 90 days of simultaneous injection of effluent in three wells at a rate of 4.0 million gallons per day and then equal rate withdrawal of 4.0 million gallons per day until the pumped water in each well reached a dissolved-solids concentration of 1,500 milligrams per liter. A recovery efficiency of 14.8 percent was

estimated for the base simulation. Ten successive injection and recovery cycles increased recovery efficiency to about 56 percent. Based on model simulations for hypothetical conditions, recovery efficiency (1) increased with successive injection and recovery cycles; (2) increased when the volume of injectant increased; (3) decreased when storage time increased; (4) did not change significantly when the injection rate or recovery rate increased, or when the ratio of recovery rate to injection rate increased, and (5) was not significantly affected by any particular geometric arrangement of wells or by the number of wells when the volume of water injected remained constant. Recovery efficiency from multiple wells was nearly the same as from a single well. Recovery efficiency ranged from about 7 to 56 percent, in several tests.

Sensitivity of recovery efficiency to variations in selected parameters such as dissolved-solids concentration of the injection zone, permeability, vertical anisotropy, longitudinal and transverse dispersivities, and effective porosity was tested. Changes in the dissolved-solids concentration of the injection zone produced the greatest change in recovery efficiency. Uniform changes in dispersivity values produced the second greatest change in recovery efficiency. Generally, recovery efficiency increased when the above parameter values were decreased and recovery efficiency decreased when these parameter values were increased.

Density difference between native and injected waters was the most important factor

affecting recovery efficiency in this study. For the base simulation, sensitivity tests indicated that recovery efficiency increased from about 15 to 78 percent when the dissolved-solids concentration of the native water decreased from about 7,800 to 500 milligrams per liter.

Dispersivity is another important factor affecting recovery efficiency. For the base simulation, sensitivity tests indicated that recovery efficiencies from about 9 to 24 percent can be obtained for different dispersivity values. A field determination of dispersivity was not made as part of this study, and values used may not be representative of the actual dispersive characteristics of the aquifer system at the study site. However, dispersivity values tested are within the range of values used in previous studies.

INTRODUCTION

The city of St. Petersburg owns and operates one of the largest urban reclaimed water reuse systems in the world. In 1995, approximately 21 Mgal/d of advanced secondary-treatment plant effluent was piped from the city's four water reclamation facilities (WRF's) through a 260-mi irrigation system to water residential, recreational, and commercial properties.

Demand for reclaimed water is seasonal. There is a deficiency of effluent for irrigation in the dry months (generally fall and spring) and an excess in the wet months (generally summer and winter). The excess is disposed of through deep underground injection wells into the lowermost zones of the Upper Floridan aquifer (a highly-fractured dolomite zone saturated with saltwater). The injected water from these deep permeable zones cannot be effectively recovered because of excess mixing occurring in the disposal zone (Hickey and Ehrlich, 1984).

Developing alternate methods for augmenting water supplies is a major priority for water managers. For this reason, the U.S. Geological Survey (USGS), in cooperation with the city of St. Petersburg and the Southwest Florida Water Management District (SWF-WMD), began a study in 1994 to assess the feasibility of subsurface storage and recovery (SSR), otherwise known as aquifer storage and recovery, of effluent in a shallow, moderately transmissive limestone aquifer

underlying St. Petersburg that is slightly to moderately saline.

The objective of this study was to provide an assessment of the potential for SSR in St. Petersburg. The study included two phases:

- (1) development and testing of a prototype cylindrical numerical model to assess the recovery efficiency for injected water of a typical single well system in St. Petersburg; and,
- (2) development and testing of a three-dimensional numerical model to assess the recovery efficiency for injected water using multiple wells at one of the four St. Petersburg's WRF's.

The phase 1 single-well cylindrical model was described by Yobbi (1996). That model was devised to evaluate recovery of injected water at a typical SSR well and to assess the relation between recovery efficiency and uncertainties in values of physical properties and operational variables. For practical ranges of hydraulic and fluid properties in the study area, the model analysis indicated that (1) the greater the density contrast between injected and resident formation water, the lower the recovery efficiency, (2) recovery efficiency decreased significantly as dispersion increased, (3) high permeability produced low recovery efficiencies, and (4) recovery efficiency increased as anisotropy increased and as porosity decreased. The recovery efficiency ranged from about 4 to 76 percent in several hypothetical tests performed with the single-well cylindrical model.

An implementation of SSR would probably require more than one well to handle the required inflow rates and wellhead pressures. Operational field tests of this size are generally too expensive for preliminary assessments. Modeling is a cost-effective approach for preliminary evaluation of the feasibility of SSR since many combinations of conditions can be investigated with relatively inexpensive computer simulations.

Purpose and Scope

This report presents the results of the development of the phase 2, three-dimensional numerical model and the results of an assessment of the potential for SSR using multiple wells at the Southwest St. Petersburg WRF. Specifically, the model was used as a simulation tool to assess: (1) recovery efficiencies for injected water for multiple-well configurations,

injection and recovery rates, volumes of injected water, injection/recovery ratios, length of storage times and background hydraulic gradients, and repeated cycles, and (2) the relation between recovery efficiency and the uncertainty in values for physical properties. This report also presents numerical analysis of hydraulic properties using the model. Data were obtained from published reports and from files of the USGS.

A finite-difference model, HST3D (Kipp, 1987, as modified), for simulating heat and solute transport in three dimensions was used for the simulations. The model is used to simulate a hypothetical injection and recovery operation at the Southwest St. Petersburg WRF. Approximately 75 simulations were run and recovery efficiencies were calculated for various SSR tests. Hydrologic properties of the aquifer system also

were estimated using numerical simulation of data collected during a previous study at the Southwest St. Petersburg WRF.

Description of Study Site

The Southwest St. Petersburg WRF is located in southern Pinellas County, Florida (fig. 1). The study site is underlain by a thick sequence of honeycombed and fractured limestone and dolomite of Tertiary age overlain by a sequence of clastic deposits. Land altitudes range from about 6 to 10 ft above mean sea level.

Rainfall in the area averages about 53 in/yr, of which about 34 in. falls during the 5-month period May through September. August is the wettest month and April is the driest. The mean annual temperature

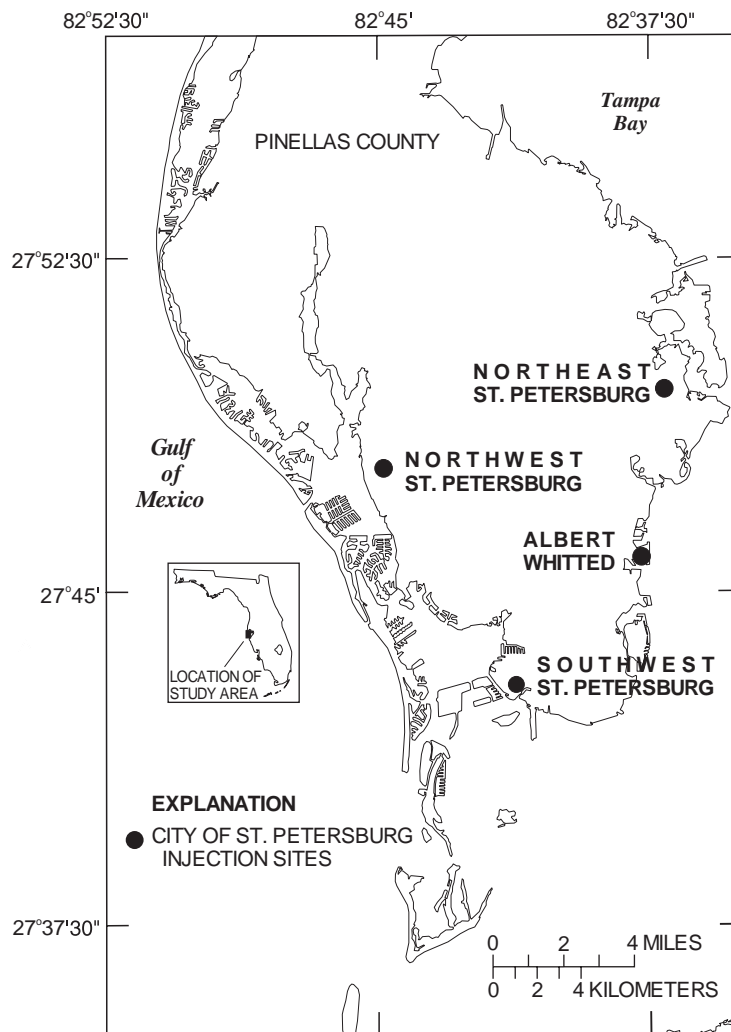


Figure 1. Location of study area and the city of St. Petersburg injection sites.

is about 74 °F, and monthly means range from about 83 °F in August to about 62 °F in January (National Oceanic and Atmospheric Administration, 1995).

Three deep injection wells comprise the injection system at the Southwest St. Petersburg WRF. The injection zone at the site is within the most productive of the identified permeable zones, with a transmissivity of about 1,200,000 ft²/d, and about 1,000 ft below land surface. The injection wells were put into continuous operation in 1979 and were designed to accept about 15.2 Mgal/d each of highly treated wastewater. In 1995, the wells were permitted for 9 Mgal/d each.

Subsurface Storage and Recovery Concept

Subsurface storage and recovery is a strategy of water-supply augmentation by which effluent is injected underground, by one or more wells, for storage during wet periods when demand is low, and then recovered later for water use during dry periods when demand is high. SSR is especially appropriate for areas like St. Petersburg where there is (1) seasonal variation in reclaimed water and demand, and (2) a moderately permeable aquifer near land surface that contains water of low to moderate salinity.

The feasibility of a SSR system depends upon the ability of the injected zone to receive, store, and discharge the injected effluent. Recovery of the stored effluent is dependent upon the effective emplacement of a relatively stable, thick lens of low-density effluent during the injection phase. To form this lens, enough effluent must be injected to displace a large volume of saline water; the mixing of the effluent and native waters must not be significant; and confinement must be sufficiently tight to prevent rapid vertical migration of the less dense effluent (Rosenshein and Hickey, 1977). The lens of effluent formed must have sufficient aerial extent and thickness to be tapped by a system of recovery wells.

The success of a SSR system is measured by the quantity of water that can be recovered relative to the quantity injected, or the recovery efficiency. Recovery efficiency, usually expressed as a percentage per cycle of injection, storage, and recovery, is defined as the quantity of water, relative to the quantity injected, that can be recovered before the water that is withdrawn fails to meet some prescribed salinity standard.

In this report, the standard is a dissolved-solids (DS) concentration of 1,500 mg/L (about 600 mg/L chloride).

Throughout this report, statements are made concerning the salinity of water. The terminology used to describe the salinity is modified slightly from a USGS-classification system of water based on dissolved solids (Heath, 1989, table 2, p. 65), as follows:

Classification	Dissolved-solids concentration (mg/L)	Percent seawater
Freshwater	<500	<1.5
Slightly saline (brackish water)	500 to 3,000	1.5 to 8.6
Moderately saline (brackish water)	3,000 to 10,000	8.6 to 29
Very saline (saltwater)	10,000 to 35,000	29 to 100
Briny	>35,000	>100

Freshwater meets the DS concentration limit for potable water. Slightly saline water is generally non-potable, but it may be suitable for irrigation. Moderately saline water is suitable for desalinization plant feed, and very saline water and briny water are considered unusable.

Factors Affecting Recovery Efficiency

Two primary physical processes affect the recoverability of the injected water: (1) mixing by molecular diffusion and hydrodynamic dispersion, and (2) density stratification. Unfavorable physical and solute properties of the aquifer system also can reduce the recoverability of injected water.

When two fluids of different composition are in contact, a transfer of molecules occurs. As time passes, the random movement of molecules creates a mixed zone where the two fluids have diffused into one another (molecular diffusion). When one fluid miscibly displaces another fluid in a porous medium, the mixed zone will be greater than that formed due to molecular diffusion alone. The additional mixing, primarily dependent on pore geometry, results from variations in the velocity field and the constant intermingling of flow paths as displacement progresses. This additional mixing, known as mechanical dispersion, occurs both longitudinally (in the direction of gross fluid movement) and transversely (in the direction normal to the gross fluid movement). Mechanical dispersion is caused by mixing of solutes due to variations in fluid velocities

resulting from local differences in hydraulic conductivity (Skibitzke and Robinson, 1963, p. B3). At the relatively large fluid velocities during injection and recovery cycles, the effects of mechanical dispersion are generally greater than those of molecular diffusion.

Density stratification describes the tendency for a lighter fluid to rise above a denser fluid. When fluids of unequal densities are in contact in a porous medium, gravity causes the less dense fluid to rise relative to the more dense fluid. Density stratification is controlled by several factors, including: (1) the density contrast between native and injected waters, (2) permeability of the injection zone, and (3) the thickness of the injection zone (Merritt, 1985). Stratification in porous media can be separated into two cases, static and dynamic (Kimbler and others, 1975). The static case involves no bulk flow of fluids except that arising from convective currents attributable to gravity. Dynamic stratification occurs in the presence of bulk

flow of fluids caused by the displacement of a native fluid by an injected fluid of different density.

HYDROGEOLOGIC FRAMEWORK

The hydrogeology of the St. Petersburg area has been described by Hickey (1982). The hydrogeologic units beneath St. Petersburg consist of a thick sequence of carbonate rock overlain by clastic deposits (fig. 2). The upper 1,100 ft includes the unconfined, surficial aquifer and the confined, Upper Floridan aquifer (UFA). The units are separated by the intermediate confining unit (ICU).

The surficial aquifer is the uppermost water-bearing formation and consists of sand and shell of Pleistocene age. The surficial aquifer underlying the study area is about 85 ft thick. The aquifer is a source of recharge to the Upper Floridan aquifer and is mainly used as a source of water for lawn irrigation in St. Petersburg.

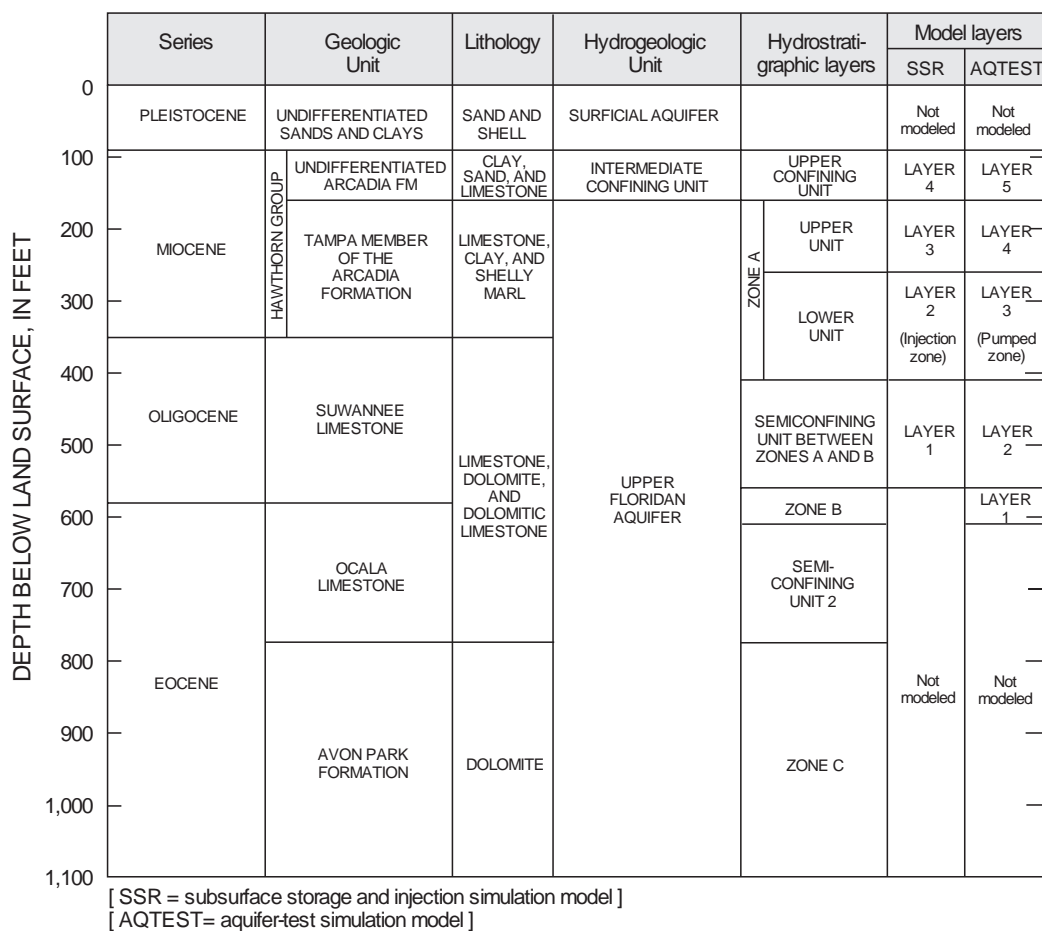


Figure 2. Generalized stratigraphic and hydrogeologic section, St. Petersburg, Florida. (Modified from Hickey, 1982.)

The low-permeable ICU lies between the surficial aquifer and the UFA. The unit coincides with the undifferentiated Arcadia Formation of the Hawthorn Group and at the study site consists of clay, sand, shell, and some limestone (Black, Crow and Eidsness, 1978). The ICU at the study site occurs at about 85 ft below land surface and is about 75 ft thick. Vertical hydraulic conductivities of the ICU range from about 3×10^{-3} to 7×10^{-5} ft/d, and average about 8×10^{-4} ft/d, as reported by Sinclair (1974). Vertical hydraulic conductivity of the ICU at the study site determined from laboratory tests is 6.9×10^3 ft/d, as reported by Black, Crow and Eidsness (1978).

The UFA is a thick, regionally extensive sequence of limestone and dolomite. The upper part consists of, in ascending order, the Avon Park Formation, Ocala Limestone, Suwannee Limestone, and the Tampa Member of the Arcadia Formation of the Hawthorn Group. Identification of three permeable zones separated by two semiconfining beds within the UFA have been listed by Hickey (1982) and include permeable zones alphabetically labeled with increasing depth from A to C. The upper part of zone A is utilized on a limited basis for irrigation and municipal water supply and zone C is used as a repository for injected treated effluent. Zones B and C contain very saline water throughout southern Pinellas County and are not utilized for any supply purposes.

Zone A is the shallowest and freshest of the producing zones and is the most promising potential receiving zone for SSR in St. Petersburg. This zone comprises the Tampa Member of the Arcadia Formation of the Hawthorn Group and the upper part of the Suwannee Limestone. Zone A occurs at about 160 ft below land surface and is about 250 ft thick at the study site. Data collected during drilling, aquifer testing, and geophysical logging indicate that zone A contains two different permeability units. The upper 100 ft of zone A is a poorly-transmissive sequence of interbedded limestone, clay, and shelly marl. The lower 150 ft of zone A is a moderately-transmissive limestone (Black, Crow, and Eidsness, 1978). Transmissivity of zone A determined analytically from data collected from an aquifer test conducted at the study site is $29,000 \text{ ft}^2/\text{d}$ (Hickey, 1982). The estimated storage coefficient of zone A (calculated from compressibility of cores and an estimated thickness of 250 ft) is 7.75×10^{-4} based on a specific storage value of 3.1×10^{-6} .

Underlying zone A is the first of a series of poorly transmissive carbonate rocks that act as semi-confining units that separate the permeable zones (Hickey, 1982). The semiconfining unit below zone A (SCU A/B) is part of the Suwannee Limestone. Thickness of the semiconfining unit at the study site is about 150 ft. The leakance coefficient of this semiconfining unit interpreted from the zone A aquifer test is $2.9 \times 10^{-3} \text{ d}^{-1}$ (Hickey, 1982).

Permeable zone B is composed of dolomite, dolomitic limestone, and limestone and includes the lower part of the Suwannee Limestone and the upper part of the Ocala Limestone. Zone B at the study site occurs at about 560 ft below sea level and is about 60 ft thick. The transmissivity, determined from specific capacity tests conducted on wells completed in zone B, is $5,000 \text{ ft}^2/\text{d}$ (Hickey, 1982).

Underlying zone B is the Ocala Limestone that acts as a semiconfining unit. This semiconfining unit at the study site occurs at about 620 ft below sea level and is about 160 ft thick. Cores from this semiconfining unit indicate that the beds have closed fractures; consequently, the unit retards the vertical movement of water between zones B and C (Hickey, 1982). Calculated vertical hydraulic conductivities range from 0.1 to 1 ft/d (Hickey, 1982).

Permeable zone C is the present repository for injected effluent. The zone is composed of dolomite, dolomitic limestone, and limestone and includes the upper part of the Avon Park Formation (Hickey, 1982). Zone C is about 320 ft thick and occurs at about 780 ft below sea level. Zone C contains the most productive water-producing intervals within the Floridan aquifer in Pinellas County. The transmissivity of zone C, based on aquifer-test analysis, is $1,200,000 \text{ ft}^2/\text{d}$ (Hickey, 1982). The storage coefficient, based on aquifer-test analysis, is 3.3×10^{-4} (Hickey, 1982). Effective porosity of zone C, determined from transport-model simulation, is 10 percent (Hickey, 1989).

NUMERICAL ANALYSIS OF HYDRAULIC PROPERTIES

A numerical ground-water flow and solute-transport model was developed to test and refine the conceptualization of the hydrogeologic system underlying the Southwest St. Petersburg WRF. Data from Hickey (1982) and interpretation of geophysical logs

and aquifer-test data were used to define the hydrostratigraphic units and to provide initial model input. The USGS computer code HST3D (Kipp, 1987, as modified) was applied using a cylindrical coordinate system. Backward-in-space and backward-in-time finite-difference equations were used in the numerical model. A brief discussion of the model is included in a subsequent section of this report.

Data were obtained from the aquifer test performed during the period of March 28 to April 1, 1977 (Hickey and Spechler, 1979) for three observation wells (B-9, B-5, and B-4, in fig. 3). A constant flow rate of 650 gal/min was maintained during the test. Results of the aquifer test indicate that water levels in

well B-9 (zone A upper unit) began to decline 60 minutes after pumping of well B-8 began and the decline in water level after 3.45 days of pumping was 1.64 ft. Water levels in well B-5 (zone A lower unit) began to decline less than one minute after pumping began and drawdown in well B-5 after 3.45 days of pumping was 1.65 ft. Water levels in well B-4 (SCU A/B) began to decline 10 minutes after pumping began and the decline after 3.45 days was 1.04 ft. The delayed response in water-level drawdown in wells B-9 and B-4 and the presence of low permeable units in the depth intervals 95-250 ft and 396-520 ft indicate the existence of semiconfining beds between producing zones (Black, Crow and Eidsness, 1978).

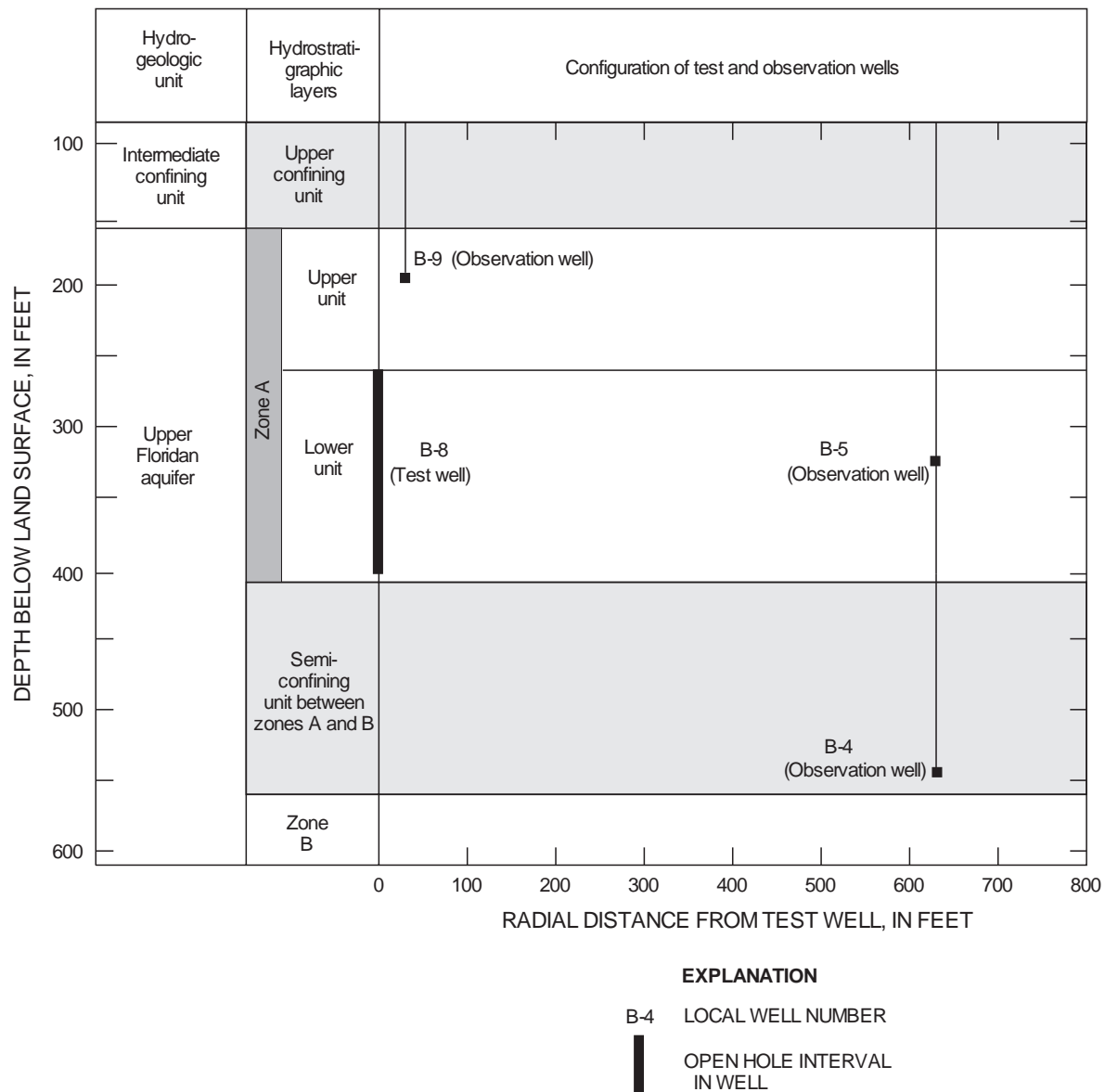
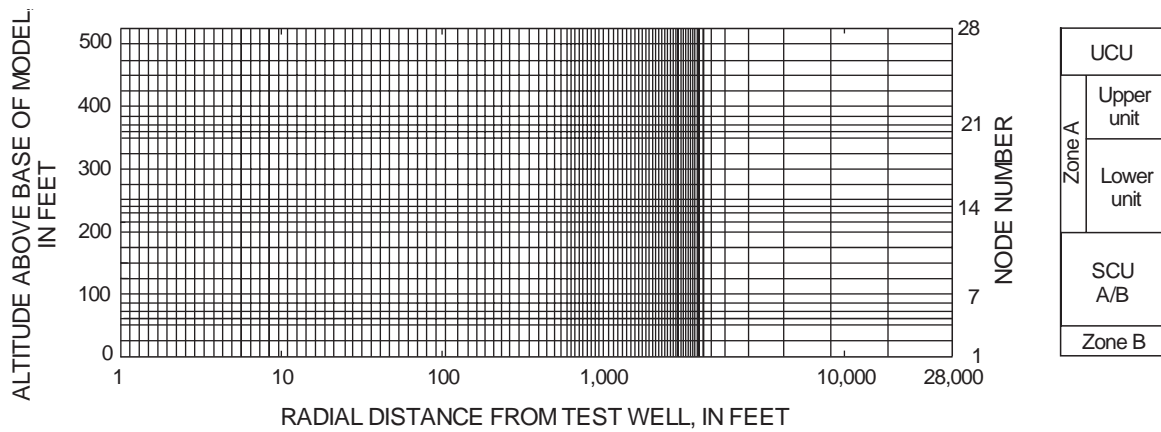


Figure 3. Generalized hydrogeologic section and configuration of test and observation wells.



EXPLANATION	
UCU	UPPER CONFINING UNIT
SCU A/B	SEMICONFINING UNIT BETWEEN ZONES A AND B

Figure 4. Cylindrical-model grid used for the simulation of hydraulic properties of the aquifer system at the Southwest St. Petersburg Water Reclamation Facility.

Model Grid and Boundary Conditions

The conceptual model consists of five layers including, from top to bottom, the upper confining unit, zone A upper unit, zone A lower unit, SCU A/B, and zone B. The model consists of 28 variable-width node spacings in the vertical direction and 97 variable-width node spacings in the radial direction (fig. 4). The model dimensions represent 28,000 ft horizontally and 675 ft vertically. The vertical spacing ranges from 10 to 25 ft. The radial grid spacings out to a distance of 105 ft present a very gradual logarithmic expansion from 0.14 ft at the well up to a maximum of 13.5 ft. With the exception of several radial grid spacings adjusted to fit the location of monitor wells, the radial dimensions of the grid from a distance of 105 ft to 2,500 ft show a constant spacing of 50 ft. The radial dimensions from a distance of 2,500 to the edge of the grid at 28,000 ft show an expansion from 100 ft to 12,800 ft.

A no-flow boundary condition was assumed at the top, bottom, outer radial edge, and the cased interval above and below the modeled withdrawal well. The no-flow boundary at the bottom of the model was deemed reasonable, because permeability is very low below the lower layer. The no-flow boundary at the top of the model was deemed reasonable, because of the distance from the withdrawal source and, because the intermediate confining bed has a hydraulic conductivity that is three orders of magnitude less than the over-

lying permeable zone. The outer radial edge boundary was intentionally located far from the withdrawal source to prevent any effect that it may have on determination of pressures in the aquifer segment affected by the withdrawal. One advantage of setting this type of boundary condition (no flow at the top, bottom, and outer edge) is that it restricts model computations to effects caused by withdrawal within a confined radially symmetrical cylinder and approximates the major flow processes during withdrawal. Both the pressure and concentration equations in the model were solved during the simulations, but only the pressure results were analyzed during calibration. Initial pressures were assumed to be hydrostatic and set on the basis of a column of water having dissolved-solids concentration specified as a function of depth. Initial solute concentrations were set equal to solute concentrations in the native water.

Calibration

Hydraulic properties of the hydrostratigraphic units were estimated from these drawdown data by using the numerical model to match simulated head changes to measured water-level changes in observation wells above, below, and within the pumped zone (zone A lower unit). The calibration focused on obtaining a satisfactory match between observed and

model-generated head change data. The model was calibrated by systematically adjusting:

- (1) hydraulic conductivity of the various units.
- (2) rock compressibility of the various units.

The time increments used to step through the model runs during calibration were gradually expanded from 1 minute to 0.54 days. A total of 16 time steps were used in the calibration. The total simulated time of pumping was 82.8 hours. The simulated well corresponds to an open hole interval from about 260 to 400 ft below land surface.

Measured drawdowns in observation wells B-4, B-5, and B-9 and the simulated drawdowns at the corresponding model nodes are shown in figure 5. Simulation results indicate that the model matched the measured responses reasonably well.

Late-time data were matched by varying hydraulic conductivity, specified in ft/d. Values of 0.0008, 0.01, 180, 0.04, and 150 ft/d for hydraulic conductivity for the upper confining unit, zone A upper unit, zone A lower unit, SCU A/B, and zone B provided the best match for late-time data.

Early-time data were matched by varying rock compressibility, specified in in²/lb. This procedure is similar to varying storage coefficient in a hydraulic model because storage coefficient (S) is considered to be a linear function of rock compressibility (C_r) according to the following formulation (Merritt, 1994):

$$S = npb(C_w + C_r) \quad (1)$$

where: S is storage coefficient (dimensionless);

n is porosity (dimensionless);

ρ is fluid density (lb/ft³);

b is layer thickness (ft);

C_w is water compressibility (3.03 x 10⁻⁶ in²/lb); and

C_r is rock compressibility (in²/lb).

Values of 5.5 x 10⁻⁵, 3.4 x 10⁻⁵, 3.4 x 10⁻⁶, 3.4 x 10⁻⁶, and 3.4 x 10⁻⁶ in²/lb for rock compressibility of the intermediate confining unit, zone A upper unit, zone A lower unit, SCU A/B, and zone B, respectively, provide the best match for early-time data.

A vector representation of the flow field generated by the model is shown in figure 6. Flow was

nearly lateral in the permeable zones and nearly vertical in the semiconfining units.

Sensitivity Analysis

A sensitivity analysis was done to evaluate the response of the model to changes in input parameters

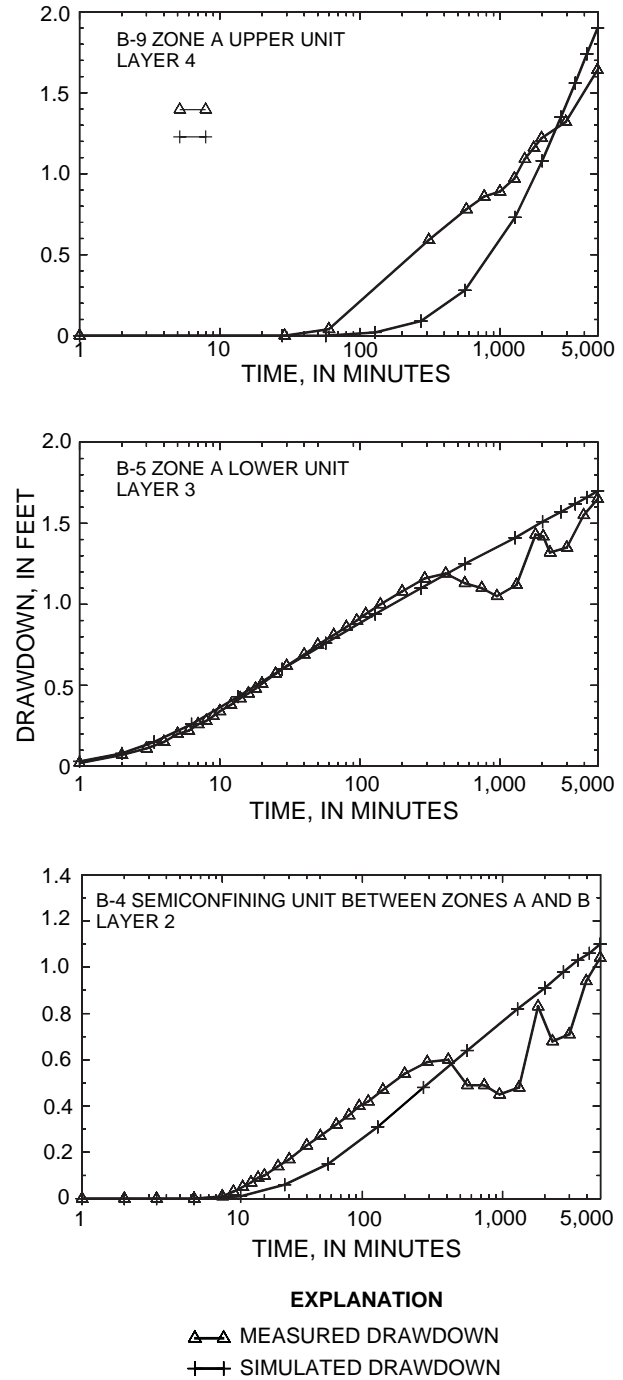


Figure 5. Simulated and observed drawdowns in wells B-9, B-5, and B-4.

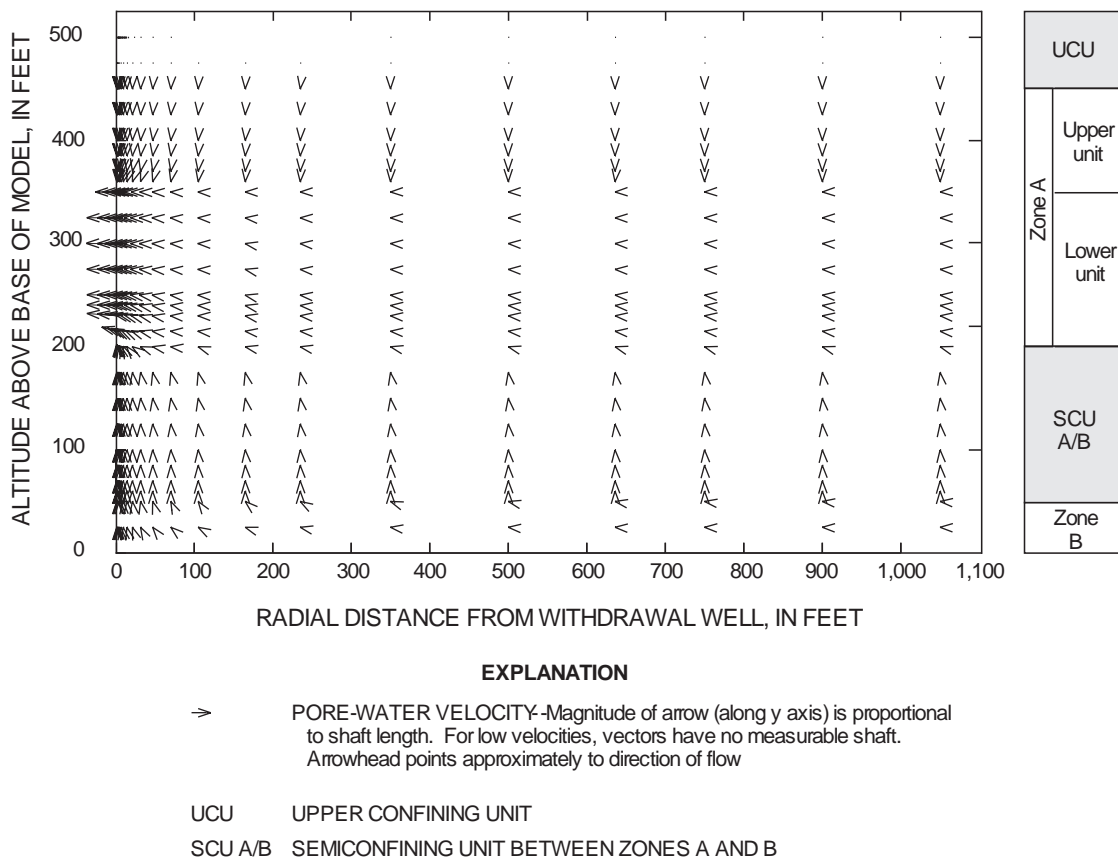


Figure 6. Simulated flow field at the end of the 3.45 day aquifer test.

and to gain an understanding of how much error could result by overestimating or underestimating the parameter values. The sensitivity analysis consisted of uniformly increasing or decreasing values of one model input parameter while others remained at calibration levels, then noting the change in drawdown as a result of the change. Hydraulic conductivity and compressibility of layers 2, 3, and 4 were increased and decreased by a factor of 10. The computed drawdowns are shown in figures 7 and 8. The tests show substantial variation from observed and simulated drawdowns at both early and late times for most of the changes.

Hydraulic Conductivity

Results of the sensitivity analysis indicate that changes in hydraulic conductivity of layer 3 (pumped zone) produced the greatest change in water levels. Generally, small changes in simulated drawdown occur when hydraulic conductivity values are increased while substantial changes in simulated

drawdown occur when hydraulic conductivity values are decreased.

If layer 2 (SCU A/B) had a much higher hydraulic conductivity than the calibrated values, hydraulic response to pumping from layer 3 would be greater than otherwise would be observed in wells B-4 and B-5 and would be smaller than otherwise would be observed in well B-9. Maximum drawdown in wells B-4 and B-9 would be about 0.3 and 0.2 ft, respectively, more than observed drawdown, and maximum drawdown in well B-5 would be about 0.1 ft less than observed drawdown.

If layer 3 (zone A lower unit) had a much higher hydraulic conductivity, water-level changes would occur much slower than observed. Hydraulic response to pumping from layer 3 in each well would be considerably more sluggish compared to the observed response. Maximum drawdowns only would be about 0.3 ft in each well, compared to 1.10, 1.70, and 1.61 ft for wells B-4, B-5, and B-9, respectively, for the calibration.

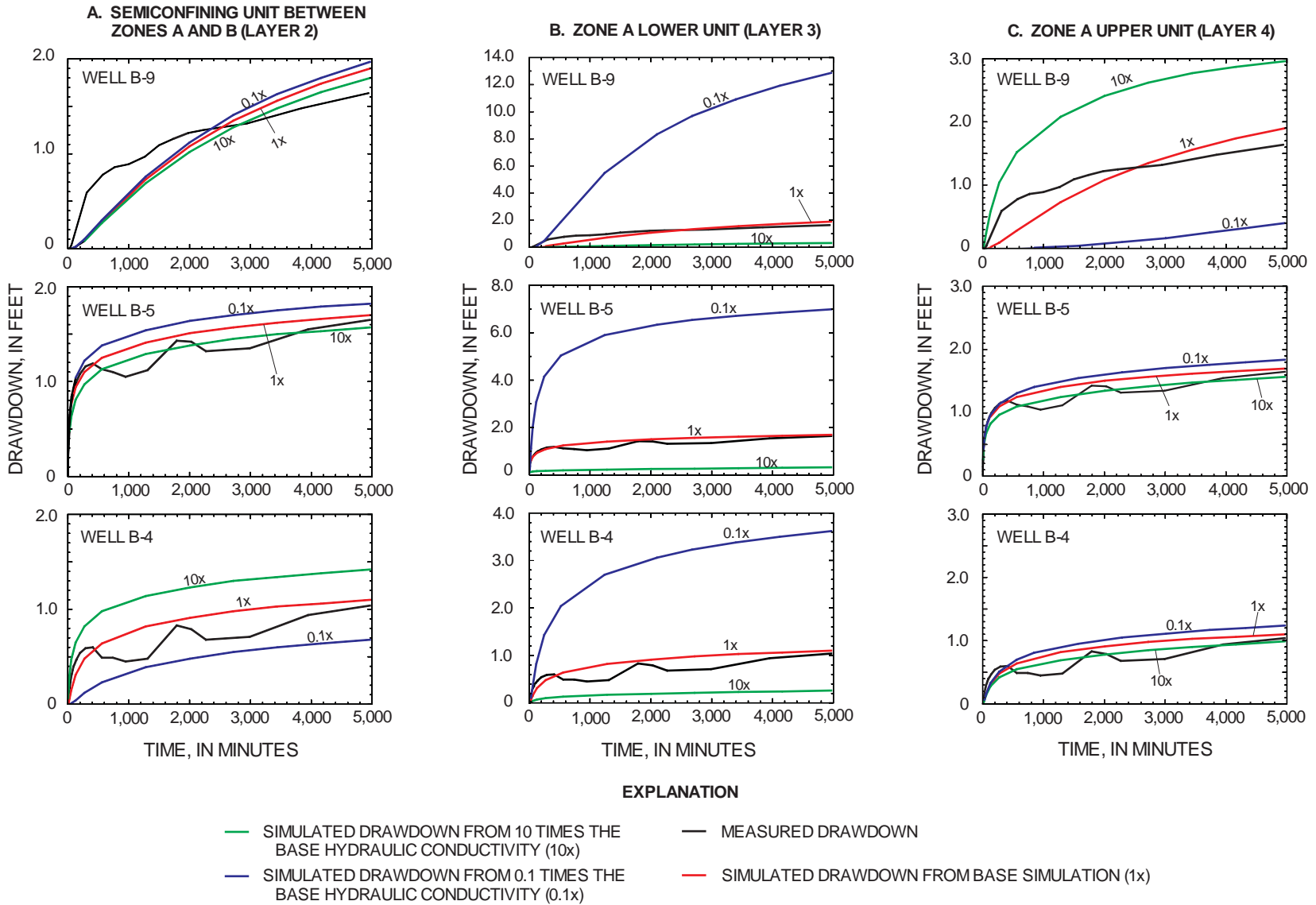


Figure 7. Effects of varying hydraulic conductivity on the simulated drawdowns in (A) semiconfining unit between zones A and B, (B) zone A lower unit, and (C) zone A upper unit.

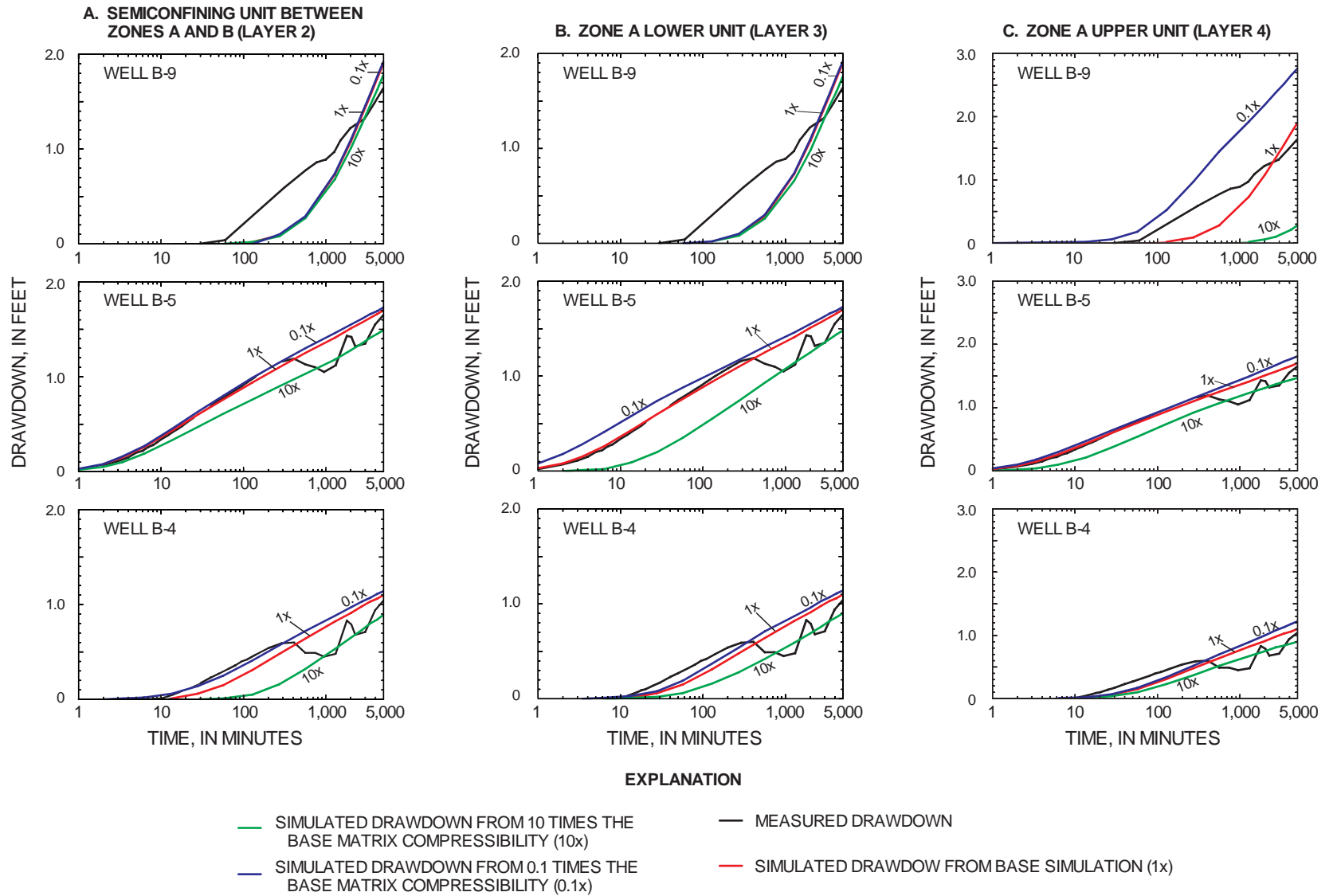


Figure 8. Effects of varying matrix compressibility on the simulated drawdowns in (A) semiconfining unit between zones A and B, (B) zone A lower unit, and (C) zone A upper unit.

If layer 4 (zone A upper unit) had a much higher hydraulic conductivity, the hydraulic response to pumping from layer 3 would be slightly less than otherwise would be observed in well B-4 and B-5 and much greater than otherwise would be observed in well B-9. Maximum drawdowns in wells B-4 and B-5 would be about 0.1 ft less than observed drawdown in each well, and maximum drawdown in well B-9 would be about 1.3 ft greater than observed drawdown.

A contrasting hydraulic response is observed when much lower hydraulic conductivity values are simulated. A tenfold decrease in hydraulic conductivity of layer 2 would result in a more responsive hydrograph than was observed in wells B-5 and B-9 and a slightly less responsive hydrograph than was observed in well B-4. Maximum drawdowns in wells B-5 and B-9 would be about 0.2 ft higher than observed, and maximum drawdown in well B-9 would be about 0.4 ft lower than observed.

A much lower hydraulic conductivity of layer 3 would result in a considerably more responsive hydrograph than was observed in each well. Maximum drawdowns would be about 2.6, 5.3, and 11.2 ft, respectively, more than was observed in wells B-4, B-5, B-9 and water-level changes would occur much faster than observed.

If layer 4 had a much lower hydraulic conductivity, the hydraulic response to pumping layer 3 would result in a slightly more responsive hydrograph for wells B-4 and B-5, and a significantly less responsive hydrograph for well B-9. Maximum drawdowns in well B-4 and B-5 would be 0.1 ft more than was observed. Maximum drawdown in well B-9 would be about 1.2 ft lower than observed, and water-level changes would occur much slower than observed.

Matrix Compressibility

Compressibility of the limestone for each layer was increased and decreased by one order of magnitude. Substantial disagreement occurred in the early-time range when this value was increased while only slight disagreement occurred in the early-time range when this value was decreased. At later times, observed and simulated data are offset to a degree that seems to change only slightly with increasing time.

If layer 2 had a much higher matrix compressibility, water-level changes would occur much slower than observed in well B-4 and slightly slower in wells B-5 and B-9. If layer 2 had a much lower matrix compressibility, hydraulic response to pumping from layer

3 in each well would be slightly quicker compared to the simulated response.

If layer 3 had a much higher matrix compressibility, water-level changes would occur much slower than observed in wells B-4 and B-5 and only slightly slower in well B-9. If layer 3 had a much lower matrix compressibility, hydraulic response to pumping from layer 3 shows only slight discrepancies with observed data at early times.

If layer 4 had a much higher matrix compressibility, the hydraulic response to pumping layer 3 would result in a significantly less responsive hydrograph than would be observed in well B-9, and only a slightly lower response than would be observed in wells B-4 and B-5. If layer 4 had a much lower matrix compressibility, water-level changes in well B-9 would occur much faster than observed while water-level changes in well B-4 and B-5 would occur only slightly faster than observed.

SIMULATION OF SUBSURFACE STORAGE AND RECOVERY OF EFFLUENT USING MULTIPLE WELLS

A finite-difference three-dimensional variable-density ground-water flow and solute-transport model was used to simulate injection and recovery from a multiwell hypothetical SSR system open to a moderately transmissive, slightly to moderately saline aquifer, underlying the Southwest St. Petersburg WRF. The specific question to be answered is: In what quantitative fashion will operational and physical variables influence recovery efficiency from multiple wells? The recovery efficiency was defined as the volume of water recovered below a dissolved-solids concentration of 1,500 mg/L (about 600 mg/L chloride), divided by the volume injected, and expressed as a percentage.

To answer this question, the USGS model HST3D (Kipp, 1987, as modified) was used to simulate the hypothetical SSR system. The analysis implemented a conceptual modeling approach (Merritt, 1985), rather than a calibration and predictive approach (Merritt, 1994), because no injection and recovery data exist for comparison with model results. This type of analysis permitted many combinations of conditions to be studied. The input values are hydraulic and native chemical characteristics of the aquifer system underlying the Southwest St. Petersburg WRF.

The rate of ground-water flow is assumed to be governed by Darcy's law, which when written in terms of fluid pressure (rather than piezometric head) is:

$$q = -k (\nabla p + \rho g z) / \mu \quad (2)$$

where,

- q is specific discharge vector (flow rate per unit cross-sectional area) [L/T];
- k is the intrinsic permeability vector of the aquifer materials [L²];
- ∇ is the gradient operator [1/L];
- p is the fluid pressure [M/LT²];
- ρ is fluid density [M/L³];
- g is gravitational acceleration vector [L/T²];
- z is the unit vector in the vertical direction [dimensionless]; and
- μ is the dynamic viscosity of the fluid [M/LT].

Using Darcy's law and the principle of conservation of fluid mass, the transport of a conservative solute can be written as:

$$\partial (n\rho) / \partial t = -\nabla (\rho q) + Q_p \quad (3)$$

where,

- n is aquifer porosity (dimensionless);
- t is time (T);
- ∇ (ρq) denotes the divergence of the specific discharge mass flux [M/(TL³)]; and
- Q_p is mass of fluid injected (+) or withdrawn (-) per unit time per unit volume of aquifer [M/(TL³)].

Numerical Model

The HST3D model (Kipp, 1987, as modified) is a computer program written in FORTRAN-77 that simulates variable density fluid movement and transport of either dissolved substances or energy in the subsurface. The HST3D version used in this report (version 2.0) is a result of several modifications made after version 1.0. In addition to changes made at the programming level to facilitate the handling of data, the main technical modification that pertains to this study is the usage of a new iterative solver (Kenneth L. Kipp, written communication, 1995). The model, as used here, solves for two interdependent variables; pressure and mass-fractional concentration in Cartesian coordinates under isothermal conditions. Backward-in-space and backward-in-time finite-difference equations are used for solution of ground-water flow

and the solute-transport equations in the numerical model. The reader is referred to Kipp's (1987) report for a complete discussion of the model code and numerical methods.

Two changes were made to the HST3D code (version 2.0). The first change was made to simulate the shutdown of the production well when the solute fraction of the withdrawn water reached 0.05769, corresponding to a DS concentration of 1,500 mg/L (about 600 mg/L chloride). The second change to the code was made to suppress the cross-derivative dispersive terms. This change was made to eliminate the nonradial spatial distribution of injectant caused by inaccuracies of the mathematical solution for radial flow in Cartesian coordinates.

Design of Base Model

The base model used as a standard for comparison for subsequent simulations was designed to be representative of the slightly to moderately saline aquifer system underlying the Southwest St. Petersburg WRF. The physical properties of the aquifer system were selected as the best possible representation of the actual field values at the study site. The chemical properties of the aquifer system were estimated values of the native formation waters prior to the start of deep well injection into zone C (about 1977). Initial pressures for the simulation were calculated by the solute-transport model on the basis of the boundaries and properties of the aquifer system.

Several simplifying assumptions are made in the conceptualization and simulation of the flow system:

1. The aquifer system is homogeneous and isotropic in all directions.
2. Hydrostatic conditions initially prevail.
3. A uniform native fluid density exists within each model layer.
4. The water-quality profile is laterally homogeneous throughout the model area.
5. The viscosity of the injected and native fluids is the same.
6. Dispersivity is constant throughout each model layer, and
7. Injection and recovery wells are 100 percent efficient.

Data from the numerical simulation discussed in the previous section were used to define the hydrogeologic system and to provide the basis for estimating the hydraulic characteristics for the aquifer system underlying the Southwest St. Petersburg WRF. The conceptual model consists of four layers representing,

from top to bottom, the upper confining unit, zone A upper unit, zone A lower unit, and the semiconfining unit between zones A and B (fig. 2).

Grid Design

To apply the HST3D model, the hydrologic and hydrogeologic characteristics of the aquifer system

underlying the study site was discretized using a Cartesian coordinate system (fig. 9). The model area dimensions are 5,000 by 5,000 horizontal ft and 475 vertical ft. The horizontal grid consists of 31 rows by 31 columns. Grid dimensions range from 100 by 100 ft at the center of the grid to a maximum of 200 by 200 ft at the four corners of the grid. The vertical grid consists of 19 intervals each 25-ft thick (20 equally spaced nodes).

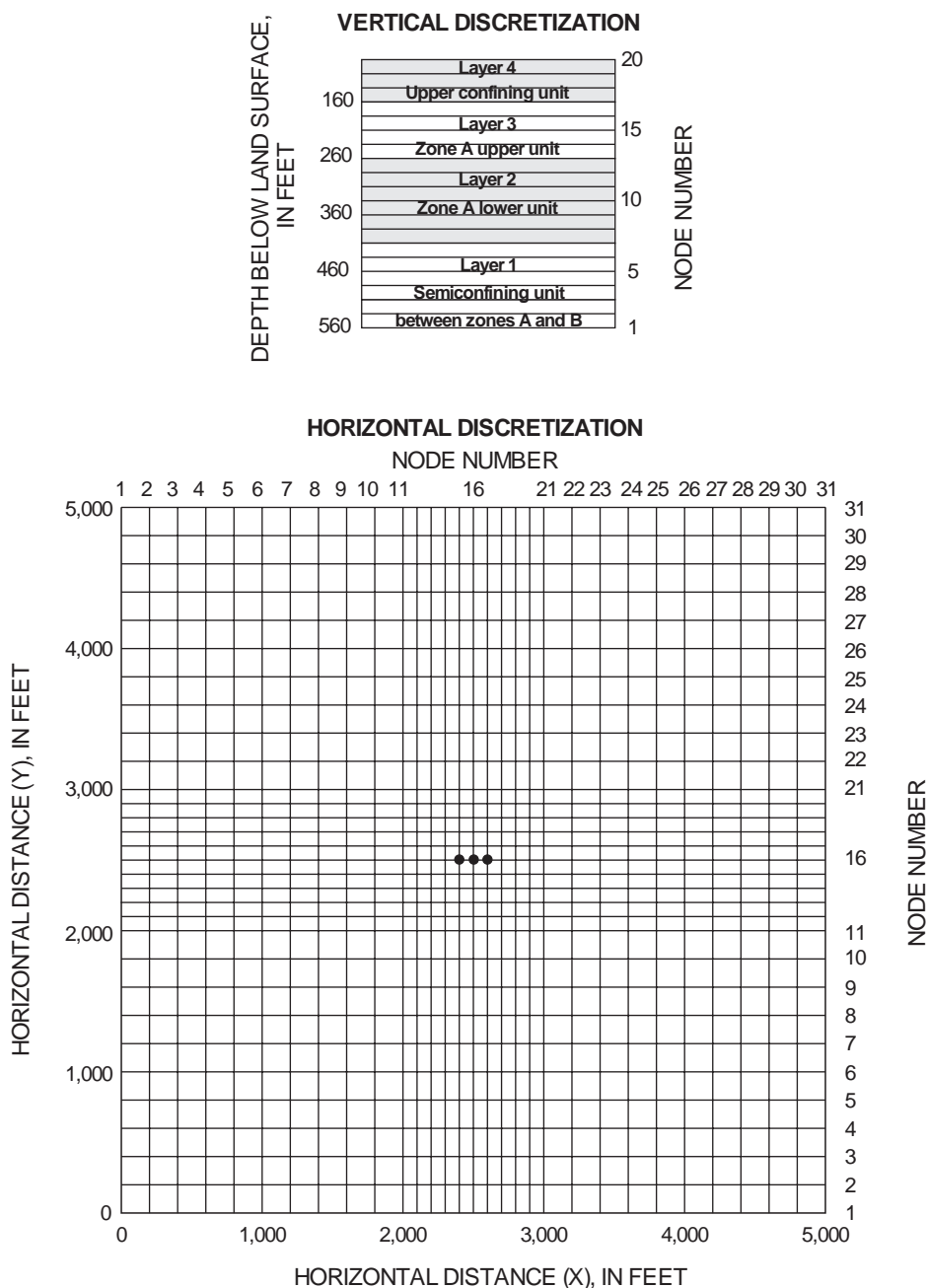


Figure 9. Vertical and horizontal discretization of the model grid used for the simulation of subsurface storage and recovery. (Position of injection/recovery wells used in the base simulation model is indicated by heavy dots.)

Boundary Conditions

Boundary conditions are used to constrain the lateral and vertical extent of the simulated flow system providing a simplified representation of the flow and transport processes at the model limits. The top and bottom boundaries of the model are specified pressure boundaries. The pressures were set equal to the hydrostatic pressures at the specific depths where the boundaries were located. Pressure on the upper boundary is set at 36.760 lb/in², equivalent to the pressure exerted from an overlying 85-ft column of freshwater presumed to exist in the overlying surficial aquifer. Pressure on the lower boundary is 243.465 lb/in², equivalent to the pressure exerted from a 560-ft column of freshwater and saline water presumed to exist in the overlying formations. One limitation of setting this type of boundary condition is that if injected or mixed water passes across these boundaries, the model would be unable to consider it during the recovery pumping. For this study, this boundary condition yielded the best representation of the actual aquifer and yielded more conservative estimates of recovery efficiency.

The lateral extent of the model is represented by leakage boundaries used to simulate flow into or out of the model at these locations. Representation of leakage-boundary conditions is based on the approach of Prickett and Lonquist (1971, p. 30-35), which has been generalized to include variable-density and variable-viscosity flow (Kipp, 1987). The leakage-boundary employed in the HST3D code accounts for permeability and thickness of the confining unit, fluid density in the outer aquifer and at the simulation-region boundary, viscosity in the confining layer, and elevation of the simulation-region boundary and the elevation at the top of the confining layer. The reader is referred to Kipp's (1987) report for a complete discussion of this boundary condition.

Fluid Properties

The fluid properties of the native formation waters assumed for the simulations are listed in table 1 and include temperature, viscosity, fluid compressibility, molecular diffusivity, and DS concentration expressed as scaled-solute mass fraction (SSMF). Isothermal conditions at 75 °F were assumed to prevail. Fluid densities assigned to

injected and native waters were based on the measured or estimated concentrations of DS concentrations in each fluid. Viscosity of the injected and native formation waters vary with temperature and solute fraction. Because isothermal conditions were assumed to prevail and because the viscosity of freshwater and saltwater differ by only 0.06 centipoise, a constant viscosity of 0.8904 centipoise (viscosity of pure water at 75 °F) was used.

Compressibility of water was held constant at $3.03 \times 10^{-6} \text{ (lb/in}^2\text{)}^{-1}$ (Freeze and Cherry, 1979, p. 52), and molecular diffusivity of the solute in the porous media was set at $9.30 \times 10^{-5} \text{ ft}^2\text{/d}$ (Kimblar and others, 1975). The model SSMF is a term ranging in value from 0 to 1. Any fluids present within or entering the aquifer system in simulation exercises are considered to be a mixture of the two fluids by the appropriate specification of SSMF values. SSMF = 0 was used to represent pure freshwater (0 mg/L), and SSMF = 1 represents the most saline native water (26,000 mg/L) residing within the aquifer system, than at the base of the model. The assigned densities of 62.2690 lb/ft³ (SSMF = 0) and 63.4582 lb/ft³ (SSMF = 1) at 75 °F and atmospheric pressure were obtained from a standard handbook (Chemical Rubber Company, 1982). The SSMF values of the injected effluent, the water of the aquifer system, and water in mixtures of effluent and native formation waters were assigned values based on their salinity relative to the two extremes. The model was simplified with the assumption of a vertically uniform initial DS concentration distribution assigned to each layer although a vertical salinity gradient has been documented (Hickey and Spechler, 1979; Hickey, 1982). SSMF values of 0.0192 (500 mg/L DS), 0.0769 (2,000 mg/L DS), 0.3005 (7,813 mg/L DS), and 0.6490 (16,874 mg/L DS) represent the composite background water quality in samples from wells at the Southwest St. Petersburg WRF injection site (Hickey and Spechler, 1979). These values were assigned to the upper confining unit, zone A upper unit, zone A lower unit and the SCU A/B, respectively. Measured injected-water DS concentration was about 700 mg/L and was assigned a SSMF value of 0.0269.

Table 1. Fluid properties assumed for simulation

[°F, degrees Fahrenheit; in²/lb, inch squared per pound; ft²/d, foot squared per day; mg/L, milligrams per liter; SSMF, solute scaled mass fraction; DS, dissolved-solids concentration]

Model unit	Hydrostratigraphic layer	Temperature (°F)	Viscosity (centipoise)	Fluid compressibility (in ² /lb)	Molecular diffusivity (ft ² /d)	SSMF (unitless)	DS (mg/L)	Water classification
Layer 4	Upper confining unit	75	0.8904	3.03 x 10 ⁻⁶	9.30 x 10 ⁻⁵	0.0192	500	fresh water
Layer 3	Zone A upper unit	75	0.8904	3.03 x 10 ⁻⁶	9.30 x 10 ⁻⁵	0.0769	2,000	slightly saline
Layer 2	Zone A lower unit	75	0.8904	3.03 x 10 ⁻⁶	9.30 x 10 ⁻⁵	0.3005	7,813	moderately saline
Layer 1	Semiconfining unit between zones A and B	75	0.8904	3.03 x 10 ⁻⁶	9.30 x 10 ⁻⁵	0.6490	16,874	very saline

Matrix Properties

Matrix properties are defined for each of the four hydrogeologic layers of the model (fig. 2, table 2). The matrix properties are intrinsic permeability, matrix compressibility, effective porosity, longitudinal dispersivity, and transverse dispersivity.

Table 2. Matrix properties assumed for simulation

[ft/d, foot per day; ft² foot squared; α_L, longitudinal dispersivity; α_T, transverse dispersivity; in²/lb, inch squared per pound]

Model unit	Hydrostratigraphic layer	Hydraulic conductivity (ft/d)	Intrinsic permeability (ft ²)	Effective porosity (unitless)	α _L (feet)	α _T (feet)	Matrix compressibility (in ² /lb)
Layer 4	Upper confining unit	0.0008	3.102 x 10 ⁻¹⁵	0.3	25.0	2.5	5.5 x 10 ⁻⁵
Layer 3	Zone A upper unit	0.01	3.878 x 10 ⁻¹⁴	0.3	25.0	2.5	3.4 x 10 ⁻⁵
Layer 2	Zone A lower unit	180	6.979 x 10 ⁻¹⁰	0.3	25.0	2.5	3.4 x 10 ⁻⁶
Layer 1	Semiconfining unit between zones A and B	0.04	1.551 x 10 ⁻¹²	0.3	25.0	2.5	3.4 x 10 ⁻⁶

Intrinsic permeability is defined as:

$$k = \mu K / \rho g$$

where,

- k is intrinsic permeability [L²];
- μ is dynamic viscosity of the fluid [M/LT];
- K is hydraulic conductivity, [L/T];
- ρ is fluid density [M/L³]; and
- g is gravitational acceleration [L/T²].

Intrinsic permeability was calculated from hydraulic conductivity values given in table 2 and conversion factors obtained from Freeze and Cherry (1979, p. 29). Values of hydraulic conductivity and matrix compressibility were based on simulation of aquifer-test data as previously discussed. The ICU was assumed to be 75 ft thick, have a hydraulic conductivity of 0.008 ft/d, and a matrix compressibility of 5.5 x 10⁻⁵ (lb/in²)⁻¹. Zone A upper unit was assumed

to be 100 ft thick, have a hydraulic conductivity of 0.01 ft/d, and a matrix compressibility of 3.4 x 10⁻⁵ (lb/in²)⁻¹. The injection zone (zone A lower unit) was assumed to be 140 ft thick, have a hydraulic conductivity value of 180 ft/d, and a matrix compressibility of 3.4 x 10⁻⁶ (lb/in²)⁻¹. The SCU A/B was assumed to be 150 ft thick, have a hydraulic conductivity of 0.04 ft/d, and a matrix compressibility of 3.4 x 10⁻⁶ (lb/in²)⁻¹.

The effective porosity of all layers was set at 30 percent, based on estimates from geophysical logs at the WRF injection sites in St. Petersburg (Hickey, 1982). The values of longitudinal (α_L) and transverse (α_T) dispersivity were not quantified as part of this study and were assumed to be 25 ft and 5 ft, respectively. These values meet gridding stability criteria recommended in Voss (1984, p. 232), where α_L and α_T are greater than one-fourth and one-tenth the spacings along and transverse to the flow direction.

Effects of Operational Factors on Recovery Efficiency

A series of hypothetical SSR tests were made for the aquifer system underlying the Southwest St. Petersburg WRF using the numerical modeling technique. A base simulation was used as the standard to study the effects of changing a series of SSR operational variables and physical properties on recovery efficiency. The effect on recovery efficiency from multiple-well configurations, rates of injection and recovery, volume of water injected, storage time and regional flow, and operational schedules were studied using the numerical model.

The general results from the analysis, which are described in the following sections, indicate that recovery efficiency improves as the volume of injectant increases and improves with successive injection and recovery cycles. Recovery efficiency decreases significantly as storage time increases due to advection and hydrodynamic dispersion. Recovery efficiency was not significantly affected by the rate of injection, by the rate of recovery, by the ratio of recovery to injection rate, by a particular multiple well geometric arrangement, or by the total number of wells used.

Base Simulation

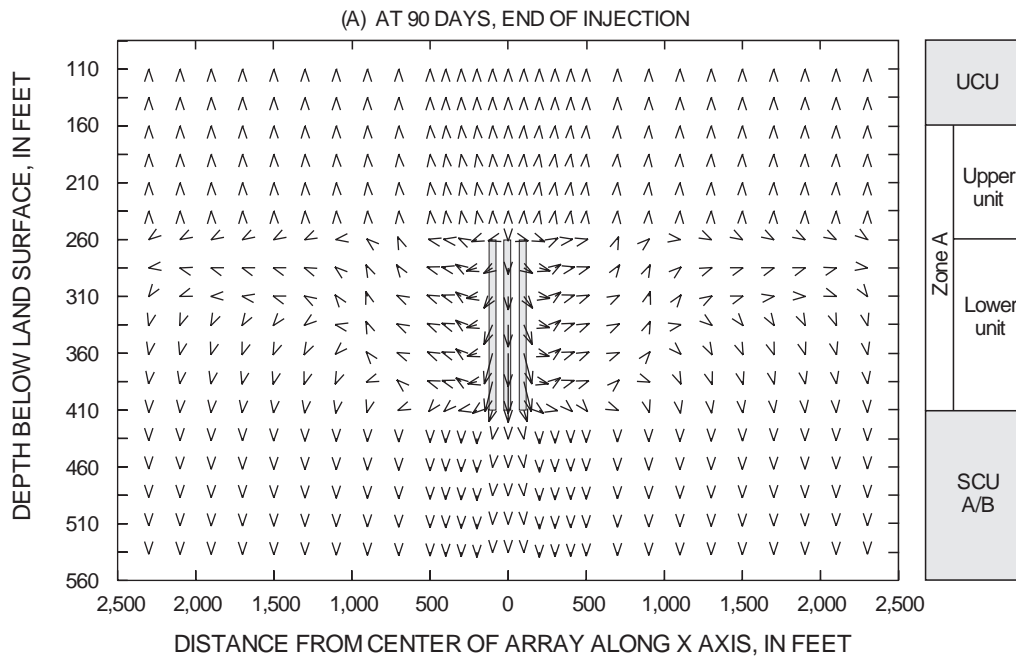
The base simulation used as a standard for comparison consisted of a single cycle of 90 days of simultaneous injection of effluent in three wells at a total rate of 4.0 Mgal/d at a temperature of 75 °F, and then withdrawal of 4.0 Mgal/d from all wells until the pumped water in each well reached a salinity limit corresponding to 1,500 mg/L DS concentration, at which time the production well was shut off. The wells are centered in the middle of the grid and aligned 100 ft apart on the X-axis. For the base simulation, a DS concentration of 1,500 mg/L was reached in 12.4 days in the two peripheral wells and 15.1 days in the center well. The recovery efficiency calculated for the base simulation is 14.8 percent.

Two simulations were made with the same parameters that were used in the base simulation; one using no-flow/no-transport boundaries at the top and bottom limits of the model, and a second

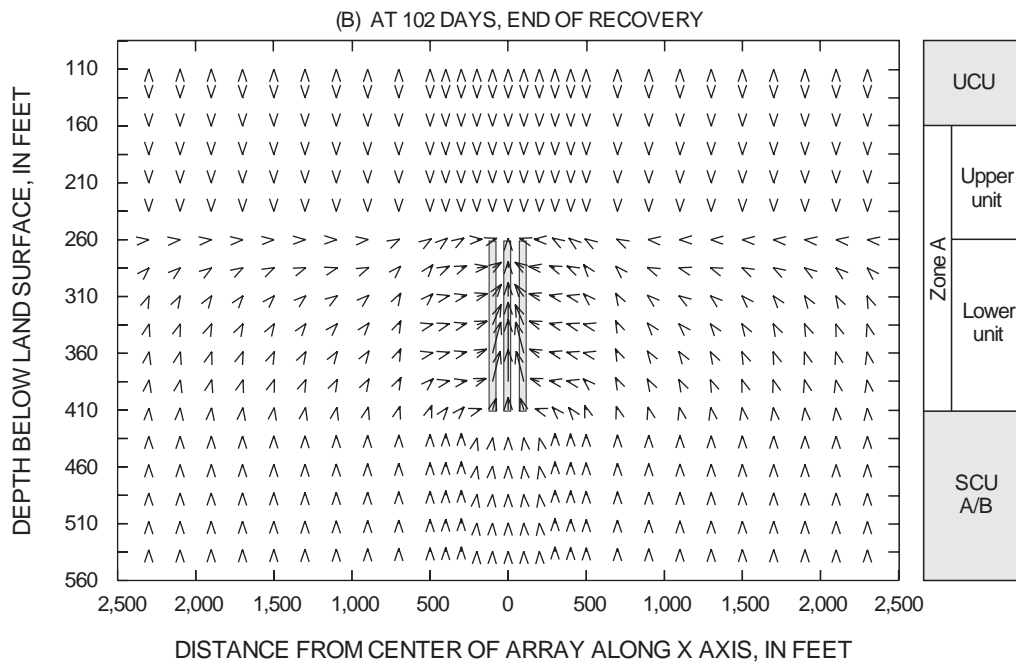
using no-flow/no-transport boundaries at the lateral limits of the model. These simulations were made to test the effect on recovery efficiency of using a constant pressure/constant concentration boundary condition at the top/bottom boundary and a leaky-aquifer boundary at the lateral boundaries to represent interlayer solute mass movement across these boundaries. The simulations yielded recovery efficiencies of 14.5 and 14.7 percent compared to 14.8 percent estimated from the base simulation. This indicates that constant pressure/constant concentration, and leaky-aquifer boundaries have a very small effect on recovery efficiency in the base simulation.

The simulated flow fields at the end of the 90-day injection simulation and at the end of the 12-day recovery phase are shown in figure 10. The general configuration of the flow field at the end of injection is typical of that of buoyant flow, where injectant mixes with and rides over the relatively denser native fluid. Flow of the injectant is along the upper part of the injection zone generally away from the center of the grid where it then is directed strongly downward beyond the leading edge of the injectant front. A similar, but opposite, flow field was generated by the model during the recovery phase.

The distribution of DS concentration associated with the flow field of figure 10 is shown in figure 11. The shape of the injectant mass is highlighted in figure 11, although vertically exaggerated, and provides an illustration of the lateral extent of the injectant mass at the end of injection and at the end of recovery. The DS concentration of the mixture increases outwardly in the transition zone between the injected effluent and native water. Figure 11A shows the upward movement of injectant above the injection wells and inward migration of more saline water in the lower part of the well. After 12 days of recovery (fig. 11B) injectant in the lower part of the wells has been depleted, although considerable injectant remains in the upper part of the wells.



UCU = upper confining unit
 SCU A/B = semiconfining unit between zones A and B



EXPLANATION

- PORE-WATER VELOCITY—Magnitude of arrow (in center of figure) is proportional to shaft length. For low velocities, vectors have no measurable shaft. Arrowhead points approximately to direction of flow.
- ▮ INJECTION WELL

Figure 10. Simulated flow field along vertical plane 16 at the end of the injection and recovery phases of the base simulation.

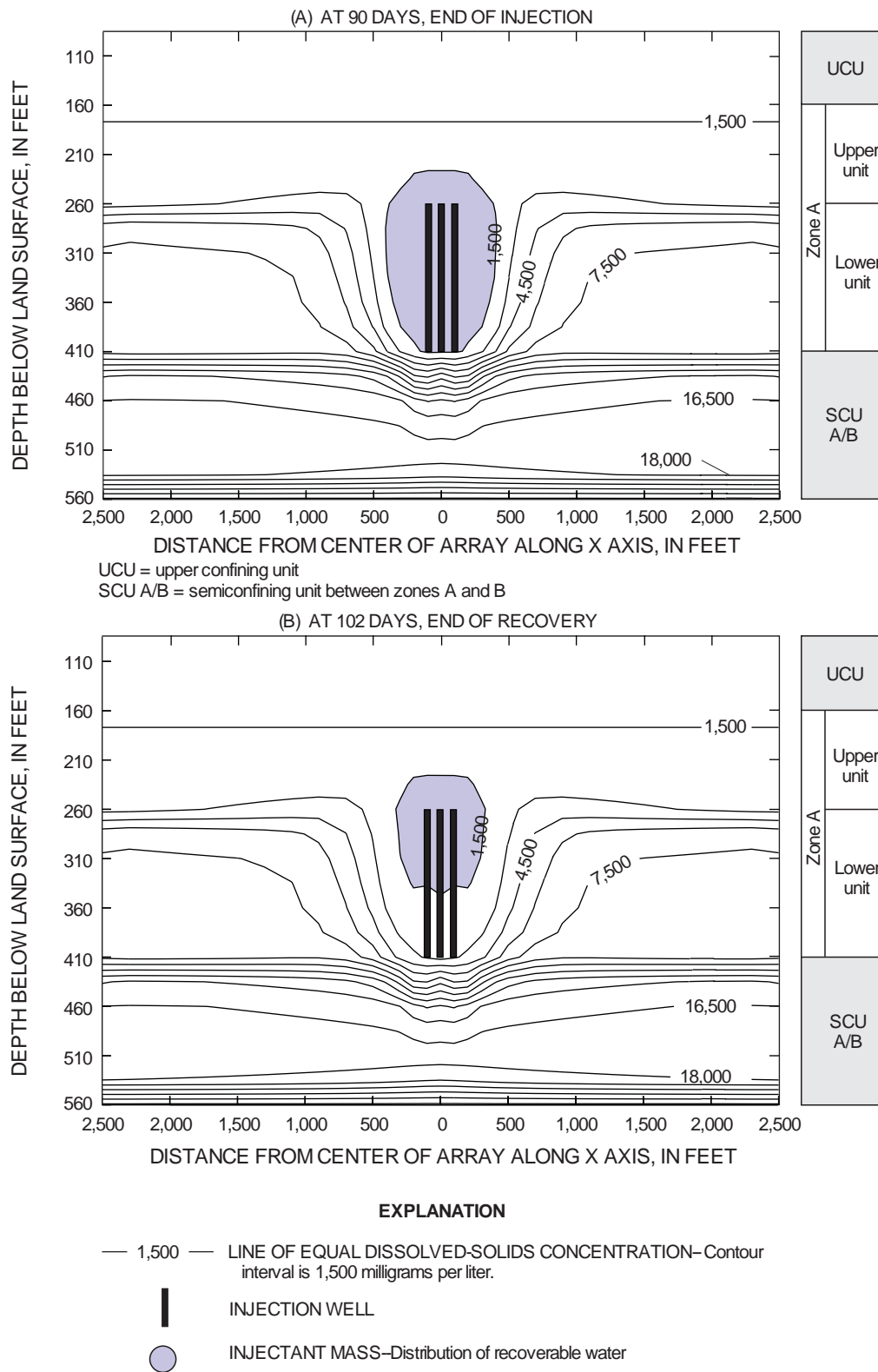


Figure 11. Simulated dissolved-solids concentration along vertical plane 16 at the end of the injection and recovery phases of the base simulation.

Multiple-Well Configurations

The effect of a group of wells on recovery efficiency was examined with ten simulations using different well configurations (fig. 12) and simultaneous equal rate injection of 4.0 Mgal/d for 90 days. Injection and recovery rates were divided equally among all

wells operating at a particular time. Withdrawal was from all wells and wells were shut off when the water withdrawn reached 1,500 mg/L. All cases were compared with a control simulation from a single well, in which computed recovery efficiency was 14.7 percent. Results of the simulations are summarized below:

Number of wells	Well configuration	Recovery time (days)					Recovery efficiency (percent)
		Well number					
		1	2	3	4	5	
1	centered in grid	13.2					14.7
2	100 ft apart on x axis	13.1	13.1				14.6
3	100 ft apart on x axis (base)	12.4	15.1	12.4			14.8
3	triangle pattern	11.7	12.4	12.4			13.5
4	square array, 200 ft apart	10.9	10.9	10.9	10.9		12.1
4	square array, 100 ft apart	13.3	13.3	12.9	13.3		14.7
4	triangle array, well in center	11.9	16.1	12.2	12.2		14.6
5	square array, well in center	11.1	11.1	17.0	11.1	11.1	13.6
5	diamond array, well in center	13.4	13.4	15.5	13.4	13.4	15.4

Simultaneous injection and equal-rate withdrawals in the two-, three-, four-, and five-well systems led to no major variations upon recovery efficiency when the volume injected remained constant. Recovery efficiencies for these configurations was nearly the same as if injection and recovery had been from a single-well.

Injection and withdrawal in the square array with wells 200 ft apart produced recovery efficiency less than the base simulation by about one-fifth (from 14.8 to 12.1 percent). In the centered configurations, peripheral wells reached their salinity limit at virtually the same time, but earlier than the center well. Because of stratification and the leaky nature of the aquifer system, appreciable vertical flow of saline water into the injection zone occurred, and therefore, the geometric arrangement of the wells was not important. Model results were similar to those reported by Merritt (1985). Merritt (1985) reported that no major variations in recovery efficiency occurred in multiwell configurations when the volume injected remained constant. The number of wells varied from one to nine in Merritt's study; however, recovery efficiency was nearly the same as the single-well system.

Recovery efficiency from a particular arrangement of wells also may depend on the schedule of withdrawal at each well. Three simulations were used to study the effects of selected operational schedules on recovery efficiency. The base simulation (three-well center configuration) was the test case for comparing the withdrawal schedules. Each test consisted of four consecutive 90-day cycles of simultaneous

injections and equal-rate withdrawals at all wells. Withdrawal was from selected wells until the solute fraction of the withdrawn water at any of the wells reached a DS concentration of 1,500 mg/L. Injection and withdrawal rates were the same in all tests (4.0 Mgal/d) and were divided equally among all wells operating at a particular time. The following withdrawal schedules were simulated:

Test 1-- Withdrawal at only the center well until the perimeter wells exceeds salinity limit.

Test 2-- Withdrawal at only the center well until withdrawn water exceeds salinity limit.

Test 3-- Equal rate withdrawal at all wells until the water in the perimeter wells exceeds salinity limit.

Results of the simulations were compared to the base simulation and are summarized below:

Cycle number	Base	Test 1	Test 2	Test 3
	Recovery Efficiency			
1	14.8	13.3	14.3	13.3
2	28.7	31.2	31.2	30.0
3	37.3	40.1	40.1	39.0
4	42.8	45.0	44.8	44.8

With the exception of the first cycle, recovery efficiency for the various schedules of withdrawal was only slightly higher than that of the base simulation. The recovery efficiency increased with each cycle because residual injectant accumulated in the aquifer from previous cycles.

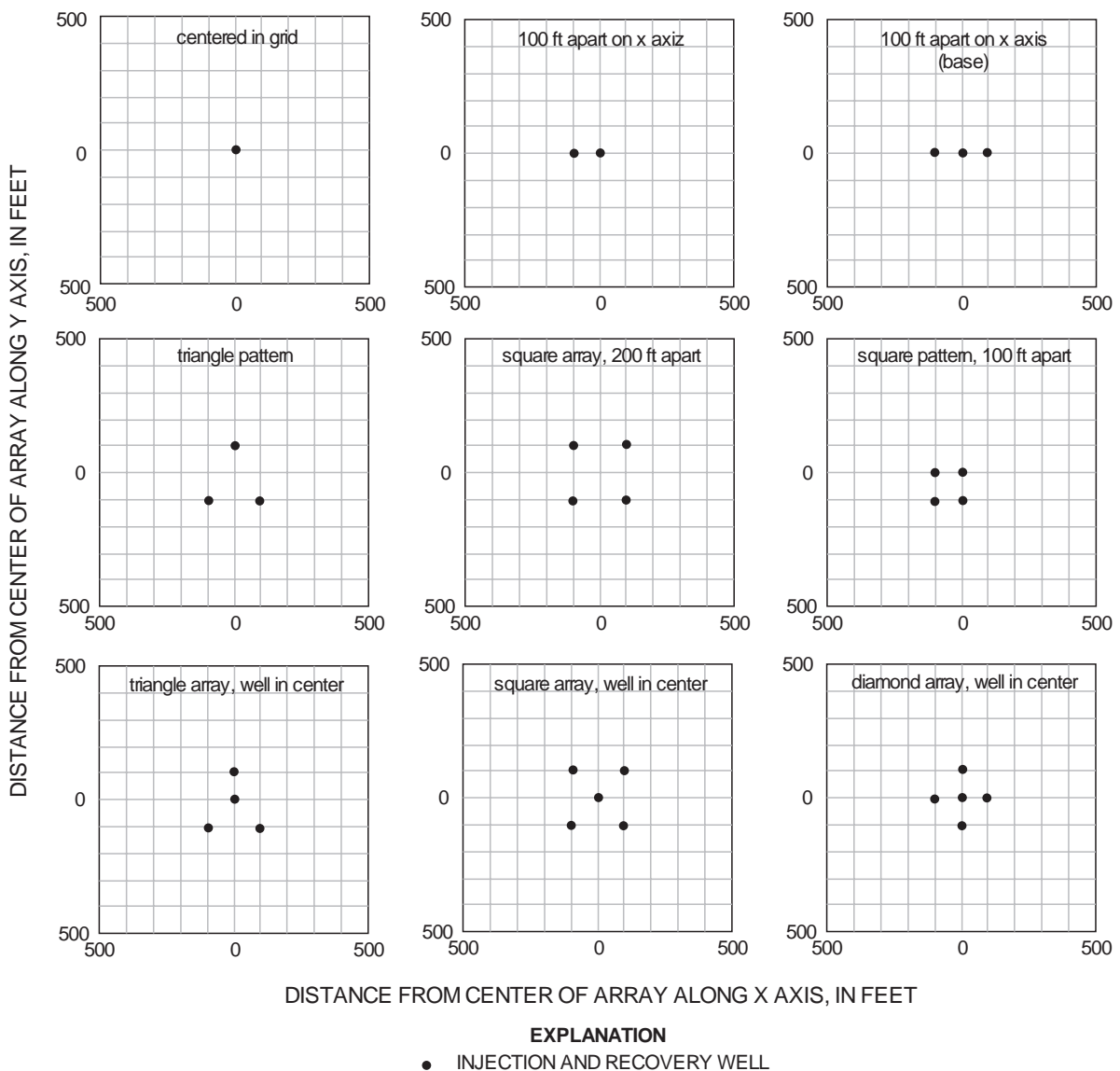


Figure 12. Geometric arrangement of injection and recovery wells.

Rates of Injection and Recovery

The base simulation model was used to simulate the injection and withdrawal of a fixed volume of water at various rates. The rate of injection and withdrawal for a fixed volume of water was varied by 0.25, 0.50, 2.0, and 4.0 times the base value. The duration of injection was adjusted so that the total volume injected remained constant at 360 Mgal. Durations of injection ranged from 22.5 days at 16.0 Mgal/d to 360 days at 1.0 Mgal/d. Results of the simulations are summarized below:

Injection/recovery rate (Mgal/d)	Volume of water injected (Mgal)	Injection time (days)	Recovery efficiency (percent)
16.0	360	22.5	15.0
8.0	360	45.0	13.9
4.0 base	360	90.0	14.8
2.0	360	180.0	14.8
1.0	360	360.0	13.6

Results of the simulations indicate no significant relation between the rate at which a given volume of water was injected or withdrawn and the amount of water that could be recovered. This implies that the

simulated dispersion process is most sensitive to the extent of fluid movement to a new position and not to the rate of movement to that position.

The effects of using different ratios of recovery to injection rates (Q_R/Q_I) also were studied and are summarized below:

Injection rate (Mgal/d)	Recovery rate (Mgal/d)	Q_R/Q_I	Recovery efficiency (percent)
4	1	1/4	14.0
4	2	1/2	14.4
4 (base)	4	1/1	14.8
4	8	2/1	14.9
4	16	4/1	15.1

When Q_R/Q_I ratios were decreased to 1/2 and 1/4, the recovery efficiency decreased slightly from 14.8 (base simulation) to 14.4 and 14.2 percent, respectively. When the Q_R/Q_I ratios were increased to 2/1 and 4/1, the recovery efficiency increased slightly from 14.8 percent (base simulation) to 14.9 and 15.4 percent, respectively. Because the mass of injected water buoys upward, native water generally remains near the bottom of the wells, and therefore, the duration and rate of injection and recovery are not important.

Volume of Water Injected

Various changes in the volume of water injected for a fixed time period were studied in the base simulation model using six simulations in which the injected volume was varied from 0.25 to 2.0 times the base value. This was accomplished by decreasing or increasing the injection rate, while keeping the same injection time (90 days) as used in the base simulation. Zero recovery efficiency would occur for a sufficiently small injection volume because of mixing. Results of the simulations are summarized below:

Volume of water injected (Mgal)	Injection rate (Mgal/d)	Recovery efficiency (percent)
720	8.0	16.9
540	6.0	16.3
450	5.0	15.7
360 (base)	4.0	14.8
270	3.0	13.6
180	2.0	11.4
90	1.0	6.9

Simulations suggest that recovery efficiency is proportional to the injected flow volume. Recovery efficiency increased as the volume of water increased, and conversely, decreased as the volume of water decreased. For injected volumes of 1.25, 1.50, and

2.0 times the base value, recovery efficiency increased from 14.8 percent (base simulation) to 15.7, 16.3, and 16.9 percent, respectively. For injection volumes of 0.75, 0.50, and 0.25, times the base value, recovery efficiency decreased from 14.8 percent (base simulation) to 13.6, 11.4, and 6.9 percent, respectively.

Recovery efficiency increased at a greater rate at smaller volumes than at larger volumes, nearly doubling (from 6.9 to 13.6 percent) when the injection volume increased from 90 to 270 Mgal; while only increasing by about one-fifth (from 13.6 to 16.9) when the injection volume increased from 270 to 720 Mgal.

The effect of keeping the same injection rate (4.0 Mgal/d) while decreasing or increasing the injection time used in the base simulation also was tested. Results from these simulations are as follows:

Volume of water injected (Mgal)	Injection time (days)	Recovery efficiency (percent)
720	180.0	17.0
540	135.0	16.2
450	112.5	15.6
360 base	90.0	14.8
270	67.5	13.6
180	45.0	11.6
90	22.5	7.7

Results from these six simulations are similar to the previous six simulations. As discussed earlier, the dispersion process is simulated as a function of the extent of fluid movement to a new position and not the rate of movement to that position, despite the functional dependence upon flow velocity.

Storage Time and Regional Flow

Two series of model simulations were used to illustrate the effect of storage time and the effect of the regional flow in the Upper Floridan aquifer on recovery efficiency. The first series of tests consisted of five simulations using storage times of 0, 30, 90, 180, and 360 days and no regional flow. The second series of tests consisted of five simulations using storage times of 0, 30, 90, 180, 360 days and an assumed hydraulic gradient of 1 ft/mi observed at the study site. Regional flow was represented as occurring along the X-axis of the grid, and specified boundary pressure values were entered to maintain simulated flow. Results of the simulations follows:

Volume of water injected (Mgal)	Injection time (days)	Storage time (days)	Regional gradient 0 ft/mi	Regional gradient 1 ft/mi
			Recovery efficiency (percent)	Recovery efficiency (percent)
360	90	0	14.8 (base)	14.7
360	90	30	13.7	13.6
360	90	90	12.0	11.9
360	90	180	9.2	9.1
360	90	360	4.7	4.6

Simulations indicated that long storage time greatly affects recovery efficiency but shorter times do not. About a two-thirds decrease (from 14.8 to 4.7 percent) in recovery efficiency was simulated when storage time was increased from 0 to 360 days. But the difference between a storage of zero and 30 days was small. If the storage period were lengthened much beyond 360 days the remaining injectant would be nearly lost completely. Simulations also show that a regional gradient of 1 ft/mi had virtually no effect on the recoverability of the injected water, within the storage times simulated.

The simulated flow fields at the end of 30, 180, and 360 days of storage are shown in figure 13. After injection ceases, rapid stratification and upconing occurs. Oscillations of the flow field in the upper unit at 180 days of storage are due to temporal instabilities in pressure. The figures show circular convection throughout a large part of the injection zone, with counter flow of native water toward the injection well in the lower part of the injection zone. The native water then mixes with the injectant, and the mixture flows away from the injection wells in the upper part of the injection zone. Because of the leaky nature of the aquifer system represented in this model, appreciable vertical flow of saline water into the injection layer occurs from adjacent layers. The longer the withdrawal is delayed, the lower the recovery efficiency. This is a major limiting factor for SSR.

Successive Cycles of Injection and Recovery

A series of ten consecutive multicycle model simulations were used to illustrate the effects of successive cycles of injection and recovery on the recovery efficiency. As discussed earlier, the base simulation consisted of a single cycle of 90 days of simultaneous injection of effluent in three wells at a rate of 4.0 Mgal/d and then equal rate withdrawal of 4.0 Mgal/d until the pumped water in each well reached a DS concentration of 1,500 mg/L. Model results from the preceding cycle were used as initial

conditions for simulating the following cycle. Results of the simulations are shown in figure 14.

Model results are similar to those reported by Merritt, (1985), Quinones and Wexler (1995), and Yobbi (1996). Recovery efficiency per cycle increases with the total number of cycles. Recovery efficiency increases very rapidly in initial cycles, increasing from about 15 percent to about 47 percent during the first five cycles, and less rapidly in later cycles, increasing from about 49 percent to about 56 percent during the last five cycles. Results also indicate that recovery efficiency approaches an asymptote after several cycles, where little improvement of recovery efficiency occurs.

Two simulations were made with the same parameters that were used in the multicycle simulation; one using no-flow/no-transport boundaries at the top and bottom limits of the model, and a second using no-flow/no-transport boundaries at the lateral limits of the model. These simulations were made to test the effect on recovery efficiency of using a constant pressure/constant concentration boundary condition at the top/bottom boundary and a leaky-aquifer boundary at the lateral boundaries to represent interlayer solute mass movement across these boundaries for multicycle simulations. The simulations yielded recovery efficiencies of 74 and 58 percent compared to 56 percent estimated after ten cycles. This indicates that constant pressure/constant concentration boundaries are important in the determination of the recovery efficiency in multicycle simulations, while leaky-aquifer boundaries have a very small effect on recovery efficiency in multicycle simulations.

Sensitivity Analysis

A series of simulation runs that started with the base model were done to determine changes in recovery efficiency due to variations in model parameters, including DS concentration of injection zone water, permeability, anisotropy, longitudinal and transverse dispersivities, and effective porosity. The sensitivity

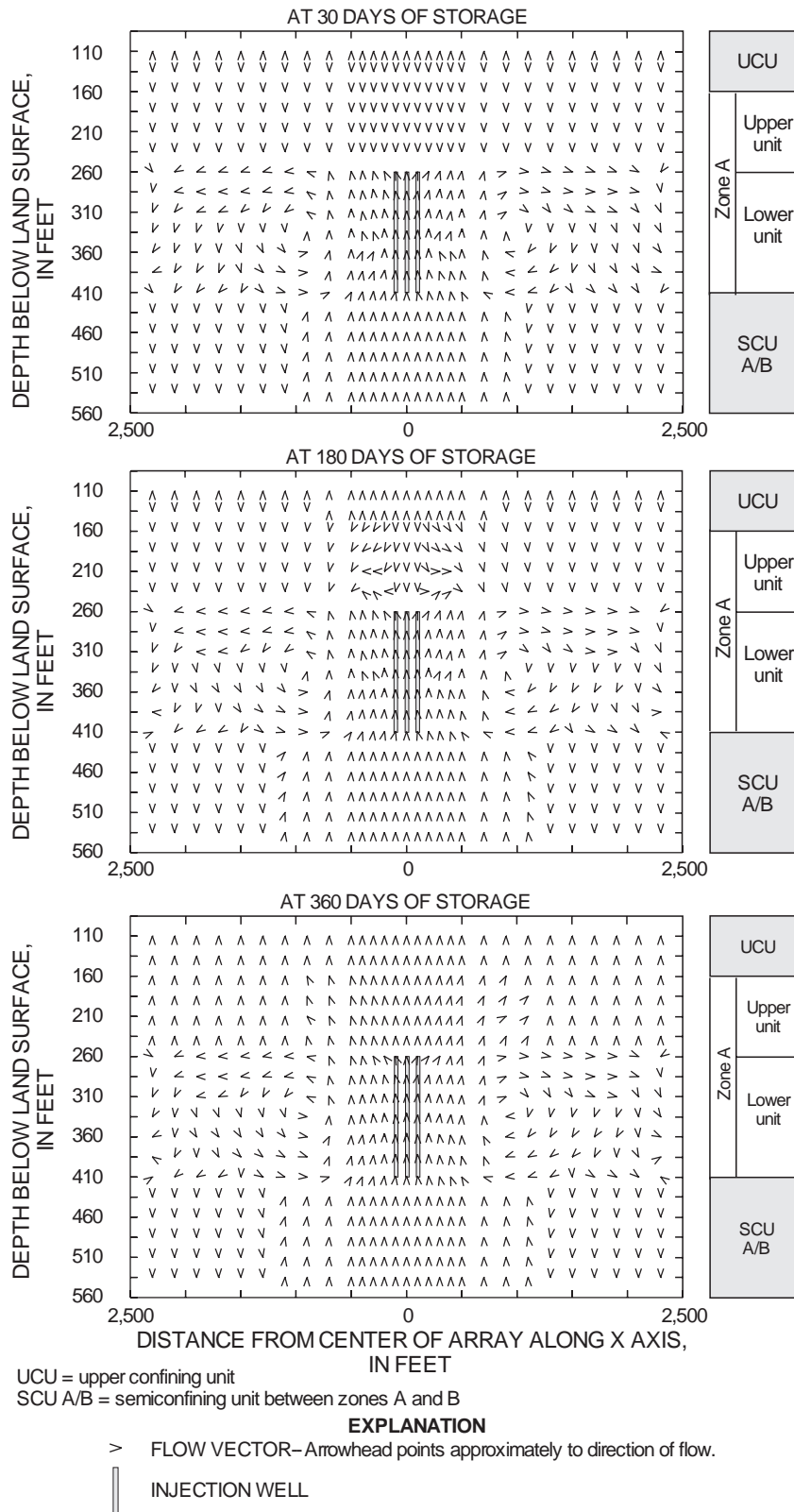


Figure 13. Simulated flow field along vertical plane 16 at the end of 30, 180, and 360 days of storage.

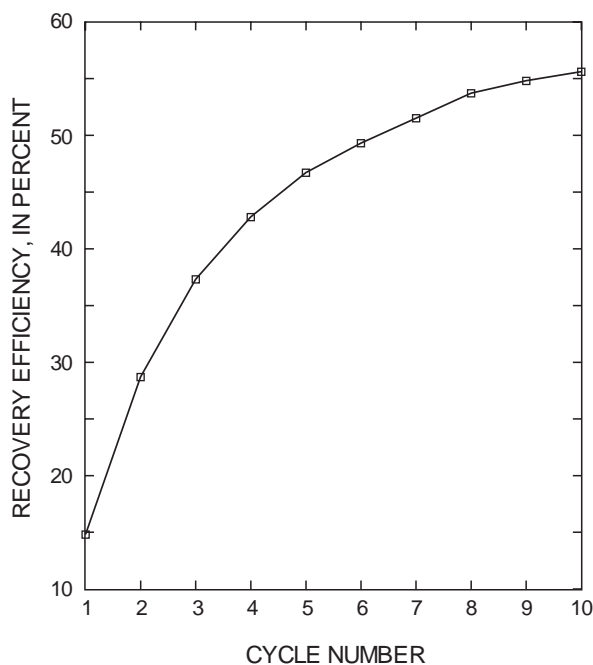


Figure 14. Recovery efficiency for ten successive injection/withdrawal cycles at 4.0 million gallons per day. (Withdrawal in each cycle ceases when the dissolved-solids concentration of water withdrawn reaches 1,500 milligrams per liter.)

analysis was conducted to assess the uncertainty of estimating selected matrix and fluid properties. For each simulation run, the value of an individual model parameter was changed by an amount that might reasonably be expected to vary from the value used in the base simulation, and noting the change in recovery efficiency as a result of the change. The simulation used as a base for comparison consisted of a single cycle of 90 days of simultaneous injection of effluent in three wells at a rate of 4.0 Mgal/d and then equal rate withdrawal of 4.0 Mgal/d until the pumped water in each well reached a DS concentration of 1,500 mg/L. A recovery efficiency of 14.8 percent was estimated for the base simulation.

The general results from the analysis, which are described in the following sections, indicate that the DS concentration of the injection zone is the most important factor, producing the greater change in recovery efficiency. The second most important factor producing significant changes in recovery efficiency is changes in longitudinal and transverse dispersivity values. Generally, recovery efficiency increased when parameter values decreased and recovery efficiency decreased when parameter values increased. The one exception is that recovery efficiency increased when

there was an order of magnitude increase in the ratio of horizontal to vertical anisotropy.

Dissolved-Solids Concentration of the Injection Zone

Simulations were made to study the effects of different DS concentration of the injection zone (zone A lower unit) on recovery efficiency. The greater the salinity of the native water, the greater will be the range of salinity across the zone of dispersion; hence, density gradients will be greater causing buoyant movement and the proportion of recoverable water within the zone will be smaller. Six DS concentrations were selected for comparison: (1) 500 mg/L, representing the least saline layer of the model; (2) 1,000 mg/L, an arbitrary value representing water somewhat more saline than the base value of the injection zone; (3) 2,000 mg/L, an arbitrary value representing slightly saline water, (4) 3,400 mg/L, an arbitrary value representing a mix of the least saline layer of the model and that of the composite base value of the injection zone, (5) 7,800 mg/L, representing the composite base value of the injection zone, and (6) 16,900 mg/L, representing the most saline layer.

Results of the simulations indicate recovery efficiency is highly sensitive to changes in the DS concentration of the injection zone (fig. 15A). Recovery efficiency decreases at a great rate as low DS concentrations increase, decreasing from about 77.8 to 23.6 percent when DS concentrations increased from 500 to 3,400 mg/L; but the rate of decrease is small at higher DS concentrations, decreasing from about 23.6 to 6.1 percent when the DS concentration of the injection zone increased from 3,400 mg/L to 16,900 mg/L. This analysis indicates that: (1) increases in DS concentrations of the injection zone can decrease recovery efficiency significantly, and (2) SSR is most promising when the DS concentration of the injection zone is low and least promising when the DS concentration of the injection zone is high.

Permeability

Permeability and effective porosity control the velocity of injectant flow. Uncertainty in the permeability value will affect the advective and dispersive components of the transport computations and, hence, the rate of solute transport. Generally, low permeability optimizes recovery efficiency, assuming that injection wells remain practical at low permeabilities.

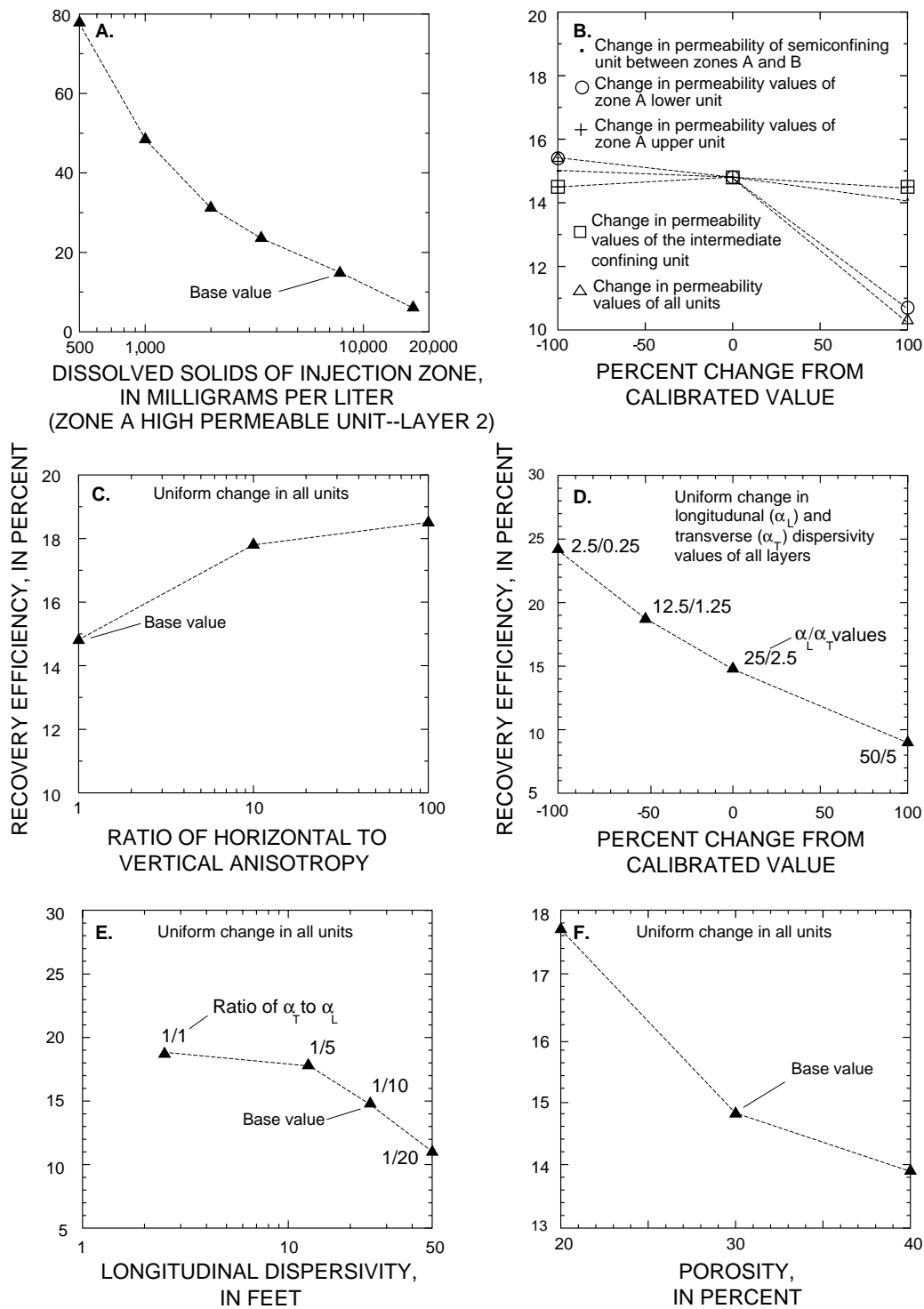


Figure 15. Relation between recovery efficiency and variations in selected model parameters.

The magnitude of permeability was changed in five different ways in the base simulation model: (1) uniform changes in all permeability values; (2) changes in permeability values of the intermediate confining unit; (3) changes in permeability values of zone A upper unit; (4) changes in permeability values of zone A lower unit; and (5) changes in permeability values of the semi-confining unit between zones A and B.

Figure 15B illustrates the variation of recovery efficiency due to permeability changes. Changes in the permeability values of all units produced the greatest change in recovery efficiency while changes in permeability values of zone A lower unit (injection zone) produced the second greatest change in recovery efficiency. Increasing permeability of the injection zone by a factor of 10 decreased recovery efficiency by about one-third (from 14.8 to 10.6 percent). The decrease in recovery efficiency is expected because of easier horizontal and vertical transport of the injected fluid, which results in greater stratification and buoyancy flow that prevents complete mixing of the injected and native waters. Also, figure 15B shows that when permeability of each layer was reduced by a factor of 0.1, recovery efficiency was not significantly affected. The major effect of the variation at lower permeability values is the increased wellhead pressure or drawdown required at the specified injection/withdrawal rate.

Anisotropy

If flow conditions vary with direction in a geologic formation, the formation is anisotropic and has differences in horizontal (k_h) and vertical (k_v) permeability. The greater the anisotropy ratio (k_h/k_v), the easier the injectant front moves along the axis of the larger permeability component. In the base simulation model, permeability is equal in all directions. To test for the effects of anisotropy, the ratio of k_h to k_v was varied from an isotropy base value ($k_h/k_v = 1$) to $k_h/k_v = 10$ and $k_h/k_v = 100$ (fig. 15C). Increasing k_h/k_v resulted in recovery efficiency increasing by about one-quarter (from 14.8 to 18.5 percent). Recovery efficiency increases because simulation of a larger k_h/k_v causes more lateral flow and inhibits upward movement of buoyant injectant.

Dispersivity

Dispersivity is a scale-dependent property of the porous medium that controls the mixing of injected and native formation fluids at their interface. When dispersivity is increased, more mixing occurs and a widening of the transition zone between the injectant and native formation waters occurs. Dispersion is a restrictive process that can severely limit recovery efficiency (Merritt, 1985).

Two different tests of the base model were made for the α_T and α_L values. In the first test, both dispersivity values were simultaneously changed by the same percentage, keeping the ratio of α_T to α_L equal to 1/10. In the second test, the ratio of α_T to α_L was changed by keeping the α_T value constant while changing the α_L value.

Figures 15D and 15E illustrate results of the simulations. The analysis indicates that uniform changes in both α_T and α_L values produced more significant changes in recovery efficiency than when the ratio of α_T to α_L was changed. Increasing α_T and α_L uniformly by 100 percent decreased recovery efficiency by about one-third (from 14.8 to 9.0 percent); while decreasing α_T and α_L uniformly by 100 percent increased recovery efficiency by about two-thirds, from 14.8 to 24.2 percent. When α_L was decreased from 25 to 2.5 ft (α_T to $\alpha_L = 1/1$) recovery efficiency increased by about one-quarter, from 14.8 to 18.7 percent. When α_L was increased from 25 to 50 ft (α_T to $\alpha_L = 1/20$) recovery efficiency decreased by about one quarter, from 14.8 to 11.0 percent. In both cases, recovery efficiency decreases as dispersivity increases. A large rate of decrease in recovery efficiency is shown as the dispersivity value or ratio of α_T to α_L , increases from low values, but the rate of decrease is small at larger dispersivity values or ratios.

Effective Porosity

Effective porosity is part of the ground-water hydraulic equation and the advective-dispersive solute-transport equation. In addition to the effect on the storage term for the transport equation, the effective porosity value is combined with the specific discharge (obtained from the ground-water flow equation) to determine the average pore-water velocities, which are used to represent the advection term in the transport equation (Quinones and Wexler, 1995).

Effective porosity of the aquifer material was tested at 20 and 40 percent to bracket the base model value of 30 percent. Figure 15F illustrates the variation of recovery efficiency due to changes in porosity. Increasing porosity caused recovery efficiency to decrease slightly, from 14.8 to 13.9 percent, whereas decreasing porosity caused recovery efficiency to increase by about one-fifth, from 14.8 to 17.7 percent. The greater the porosity, the slower the solute front will move; thus, the longer the time it takes to replace the volume of native formation water in a given volume of the aquifer and the greater the dispersive mixing. Low porosity has the opposite effect.

SUMMARY AND CONCLUSIONS

A model-based study of subsurface storage and recovery (SSR) was made to assess the potential for SSR using multiple wells at the Southwest St. Petersburg WRF. SSR is a strategy of water conservation used to augment existing water supplies. The study was specifically aimed toward applying a density-dependent, ground-water and solute-transport model to assess various operational variables and physical properties on recoverability of injected effluent.

The hydrogeologic framework used for this study was developed from interpretations of data from previous studies. The sediments underlying the study area form a sequence of two aquifers and one confining unit. The framework includes the unconfined surficial aquifer, and the confined Upper Floridan aquifer. The units are separated by the intermediate confining unit.

General aquifer characteristics were estimated from field and laboratory data including drillers logs, aquifer tests, and geophysical logs collected from previous studies. Hydraulic properties of the hydrostratigraphic units were estimated using numerical simulation of aquifer-test data. A cylindrical numerical model was calibrated by obtaining a satisfactory match between observed and model-generated head change data.

A three-dimensional numerical model of variable density ground-water flow and solute transport (HST3D) was used to evaluate the effects of changing various operational parameters on recovery efficiency of treated effluent stored in a saline aquifer underlying the study site using multiple wells. About 75 hypothetical tests of SSR were made to evaluate the effi-

ciency of this operation in the study area. A base simulation of simultaneous injection of 4 Mgal/d in three wells for 90 days and then withdrawal of 4 Mgal/d from all wells until the pumped water exceeded a dissolved-solids concentration of 1,500 mg/L was used as a reference to compare the effects of changing selected operational factors on recovery efficiency. A recovery efficiency of 14.8 percent was estimated for the base simulation. The effects of the following operational factors were assessed using the model:

1. multiple-well configurations;
2. rates of injection and recovery;
3. volume of water injected;
4. storage time and regional flow, and
5. successive cycles of storage and recovery.

Simulation results for hypothetical conditions indicate that recovery efficiency increases when the volume of injectant increases; increases with successive injection and recovery cycles, and increases slightly when the ratio of recovery rate to injection rate increases. Recovery efficiency decreases significantly when the storage time increases significantly and decreases slightly when the ratio of recovery rate to injection rate decreases. Recovery does not change significantly when the rate of injection increases or decreases.

Model results show that recovery efficiencies of about 7 to 17 percent can be achieved for different SSR operational schemes. Ten successive injection and recovery cycles can increase the recovery efficiency to about 56 percent. Other results indicate that recovery efficiency does not improve significantly in particular geometric arrangement of wells or number of wells when the volume of water injected remains constant. Recovery efficiency for the various configurations tested was nearly the same as if injection and recovery had been from a single well.

Sensitivity analysis were performed to determine changes in recovery efficiency to variations in model parameters, including:

1. dissolved-solids concentration of the injection zone,
2. permeability,
3. anisotropy,
4. dispersivity, and
5. effective porosity.

The general results from the analysis indicate that changes in the dissolved-solids concentration of

the injection zone produced the greatest change in recovery efficiency. Uniform changes in dispersivity values produced the second most significant change in recovery efficiency. Generally, recovery efficiency increased when each parameter value decreased and recovery efficiency decreased when each parameter value increased.

Density differences between native and injected waters were the most important factor affecting recovery efficiency in this study. High salinity of native water at a given permeability level permits rapid buoyancy stratification and brings about a substantial loss of recovery efficiency. Simulation results indicated that recovery efficiency decreased rapidly when the dissolved-solids concentration increased, decreasing from about 77.8 to 23.6 percent when dissolved-solids concentration increased from 500 to 3,400 mg/L.

Dispersivity is an important factor to the model sensitivity and is a restrictive process that can severely limit recovery efficiency. However, the dispersivity values used for this model were not field tested and may not be representative of the actual dispersive characteristics of the aquifer system at the study site.

SELECTED REFERENCES

- Black, Crow, and Eidsness, Inc., 1978, Drilling and testing of the monitoring and injection wells at Southwest Wastewater Treatment Plant for the city of St. Petersburg, Florida: Consultant's report in files of the city of St. Petersburg, Fla.
- Chemical Rubber Company, 1982, CRC Handbook of chemistry and physics (63rd ed): Boca Raton, Fla., CRC Press.
- Freeze, R.A., and Cherry, J.A., 1979, Groundwater: Englewood, N.J., Prentice-Hall, 604 p.
- Heath, Ralph C., 1989, Basic ground-water hydrology: U.S. Geological Survey Water-Supply Paper 2220, 84 p.
- Hickey, J.J., 1982, Hydrogeology and results of injection tests at waste-injection test sites in Pinellas County, Florida: U.S. Geological Survey Water-Supply Paper 2183, 42 p.
- , 1989, Circular convection during subsurface injection of liquid waste, St. Petersburg, Florida: Water Resources Research, v. 25, no. 7, p. 1481-1494.
- Hickey, J.J., and Ehrlich, G.G., 1984, Subsurface injection of treated sewage into a saline-water aquifer at St. Petersburg, Florida--Water quality changes and potential for recovery of injected sewage: Ground Water, v. 22, no. 4, p. 397-405.
- Hickey, J.J., and Spechler, R.A., 1979, Hydrologic data for the southwest subsurface-injection test site, St. Petersburg, Florida: U.S. Geological Survey Open-File Report 78-852, 104 p.
- Kimbler, O.K., Kazman, R.G., and Whitehead, W.R., 1975, Cyclic storage of freshwater in saline aquifers: Louisiana Water Resources Institute Bulletin 10, 78 p., with appendixes.
- Kipp, K.L., 1987, HST: A computer code for simulation of heat and solute transport in three-dimensional ground-water flow systems: U.S. Geological Survey Water-Resources Investigations Report 86-4095, 519 p.
- Merritt, M.L., 1985, Subsurface storage of freshwater in south Florida: A digital model analysis of recoverability: U.S. Geological Survey Water-Supply Paper 2261, 44 p.
- , 1994, Tests of subsurface storage of freshwater at Hialeah, Dade County, Florida, and digital simulation of the salinity of recovered water: U.S. Geological Survey Open-File Report 93-155, 112 p.
- National Oceanic and Atmospheric Administration, Climatological data, Florida, monthly summaries, 1995.
- Quinones-Aponte, Vicente, and Wexler, Eliezer J., 1995, Preliminary assesment of injection, storage, and recovery of freshwater in the lower Hawthorn aquifer, Cape Coral, Florida: U.S. Geological Survey Water-Resources Investigations Report 94-4121, 102 p.
- Pricket, T.A., and Lonquist, C.G., 1971, Selected digital computer techniques for groundwater resources evaluation: Urbana, State of Illinois, Department of Registration and Education, Illinois State Water Survey ISWS-71-BUL-55, 62 p.
- Sinclair, W.C., 1974, Hydrogeologic characteristics of the surficial aquifer in northwest Hillsborough County, Florida: Florida Bureau of Geology Information Circular no. 86, 98 p.
- Skibitzke, H.E. and Robinson, G.M., 1963, Dispersion in ground water flowing through heterogeneous materials: U.S. Geological Survey Professional Paper 386-B.
- Rosenshein, J.S., and Hickey, J.J., 1977, Storage of treated sewage effluent and storm water in a saline aquifer, Pinellas Peninsula, Florida: Ground Water, v. 15, no. 4, p. 289-293.
- Voss, C.I., 1984, A finite-element simulation model for saturated-unsaturated, fluid-density-dependent ground-water flow with energy transport or chemically-reactive single-species solute transport: U.S. Geological Survey Water-Resources Investigations Report 84-4369, p. 54-55.
- Yobbi, D.K., 1996, Simulation of subsurface storage and recovery of treated effluent injected in a saline aquifer, St. Petersburg, Florida: U.S. Geological Survey Water-Resources Investigations Report 95-4271, 29 p.

U.S. Department of the Interior
U.S. Geological Survey
227 N. Bronough St., Suite 3015
Tallahassee, Florida 32301

BOOK RATE